Am J Transl Res 2023;15(10):6264-6285
www.ajtr.org /ISSN:1943-8141/AJTR0152555

Original Article

Addition of adipose tissue-derived mesenchymal stem cells improves empagliflozin therapy for alleviating hyperglycemia–induced neuropathy

Hung-Sheng Lin[1*], Chien-Hui Yang[2*], Tsung-Cheng Yin[3], Pei-Hsun Sung[4], John Y Chiang[5], Pei-Lin Shao[6], Yi-Ling Chen[4], Chi-Ruei Huang[4], Hon-Kan Yip[4,6,7,8,9,10#], Kuan-Hung Chen[2#]

[1]Division of Neurology, Department of Internal Medicine, Kaohsiung Chang Gung Memorial Hospital and Chang Gung University College of Medicine, Kaohsiung 83301, Taiwan; [2]Department of Anesthesiology, Kaohsiung Chang Gung Memorial Hospital and Chang Gung University College of Medicine, Kaohsiung 83301, Taiwan; [3]Department of Orthopaedic Surgery, Kaohsiung Chang Gung Memorial Hospital and Chang Gung University College of Medicine, Kaohsiung 83301, Taiwan; [4]Division of Cardiology, Department of Internal Medicine, Kaohsiung Chang Gung Memorial Hospital and Chang Gung University College of Medicine, Kaohsiung 83301, Taiwan; [5]Department of Computer Science and Engineering, National Sun Yat-Sen University, Kaohsiung 80424, Taiwan; [6]Department of Nursing, Asia University, Taichung 41354, Taiwan; [7]Institute for Translational Research in Biomedicine, Kaohsiung Chang Gung Memorial Hospital, Kaohsiung 83301, Taiwan; [8]School of Medicine, College of Medicine, Chang Gung University, Taoyuan 333, Taiwan; [9]Center for Shockwave Medicine and Tissue Engineering, Kaohsiung Chang Gung Memorial Hospital, Kaohsiung 83301, Taiwan; [10]Department of Medical Research, China Medical University Hospital, China Medical University, Taichung 40402, Taiwan. [*]Equal contributors and co-first authors. [#]Equal contributors.

Received July 31, 2023; Accepted October 11, 2023; Epub October 15, 2023; Published October 30, 2023

Abstract: Background: We examined the impact of adipose-derived mesenchymal stem cell (ADMSC)-facilitated empagliflozin (EMPA) therapy for alleviating hyperglycemic induced neuropathy [i.e., diabetic neuropathy (DN)]. Methods: Study constituted N2a cell culture and rats to be classified into groups 1 (sham-operated-control)/2 (DN)/3 (DN + empagliflozin/20 mg/kg/daily orally for 6 weeks since post-day-7 DN induction)/4 (DN + ADMSCs/1.2 × 10^6 cells by vein transfusion at time intervals of 1/3/5 weeks after DN induction)/5 (DN + empagliflozin + ADMSCs) and sacrificed by day-42 after DN induction. Results: *In vitro* results showed that, compared to N2a cells, the cellular levels of senescence/DNA-damage and protein expressions of oxidative-stress (OS), apoptotic, autophagic and inflammatory biomarkers were significantly higher in N2a + glucose (25 mM) but were significantly reversed in N2a + glucose + ADMSCs, whereas the cellular levels of mitochondrial cytochrome C and protein levels of anti-oxidants displayed an opposite pattern of OS (all P<0.001). The above-mentioned parameters (i.e., OS/apoptosis/fibrosis/autophagy/DNA-damage) were lowest in N2a cells, highest in N2a + glucose and significantly higher in N2a + glucose + EMPA (50 μM) than in N2a + glucose + EMPA (150 μM) (all P<0.001). By days 7/14/21/28/35/42 after DN induction, the values of thermal paw-withdrawal-latency (TPWL)/mechanical-paw-withdrawal-threshold were highest in group 1 and significantly progressively increased from groups 2/4/3/5 (all P<0.0001). The cellular levels of unmyelinated C- and myelinated A-δ fibers, and protein levels of OS/apoptotic/DNA-damaged/fibrotic/autophagic/inflammatory/pain-facilitated/voltage-gated sodium channel biomarkers in L4-L5 levels of dorsal-root-ganglia exhibited an contradictory manner of TPWL among the groups (all P<0.0001). Conclusions: Combination of EMPA and ADMSC therapy was superior to either alone for improving outcomes of DN.

Keywords: Diabetic neuropathy, empagliflozin, mesenchymal stem cells, oxidative stress, inflammation

Introduction

The International Diabetes Federation estimates that more than 420 million people worldwide have diabetes mellitus (DM) [1, 2], indicating that DM is the largest global epidemic of the 21st century [3]. Importantly, an estimation of more than 12% of global health disbursement is directed towards DM and its care for its complications, and notably, this number is expected

to increase globally [1]. Additionally, approximately 30-50% of patients with diabetic neuropathy (DN) develop neuropathic pain (NP) [4]. The typical pathological feature of the NP is involved in the peripheral nerve, dorsal root ganglion, dorsal root, or central nervous system [2]. Although advanced pharmacological therapy for NP such as tricyclic antidepressants [5], anticonvulsants [6], opioid and atypical opioid analgesics [7, 8], the majority of patients have an unsatisfactory response to these therapies due to an unbearable painful sensation. This raises the need for a safe and efficacious management for this unresolved issue.

The underlying mechanisms of DN/chronic NP have been considerably studied as mainly through the inflammation, reactive oxygen species and mitochondria functional impairment [8-12] as well as alternation of voltage-gated sodium channel, resulting in lowering the threshold of painful sensations [11, 12]. Hyperglycemia, in addition to inducing oxidative stress chronic inflammation, and mitochondrial dysfunction in both nervous systems and neurons, also leads to activations of multiple biochemical and cellular signaling, which comprise the major source of damage in setting of DN [13].

Currently, investigators recommend that the utilization of stem cells, such as mesenchymal stem cells (MSC), could be a therapeutic option for the treatment of DN since unlike traditional pharmacological therapies, MSCs may efficaciously act through multifaceted mechanisms [14, 15]. Additionally, abundant data have shown that MSCs have several advantages: (1) easily be isolated from different tissues such as adipose-derived MSCs (ADMSCs) and can be highly expanded in vitro [15, 16]; (2) display cellular plasticity, so theoretically they could differentiate into different cell types, including neurons and Schwann cells [15, 17]; (3) begot high levels of trophic cues including neuroprotective and pro-angiogenic factors for angiogenesis and neovascularization [15, 18]; (4) could suppress the oxidative stress and inflammation [15, 19, 20]; and (5) serve as a contributor of immunomodulation. These properties raise the consideration that MSCs may post as a therapeutic option for setting of DN.

Empagliflozin (EMPA), a sodium-glucose co-transporter-2 (SGLT2) inhibitor, is approved for the management of type II diabetic patients worldwide [21]. Additionally, abundant data have clearly identified that EMPA therapy efficaciously safeguarded the kideny function i.e., to have renoprotective effects mostly independent of glycemic control in type II diabetic patients and improved the clinical outcome of cardiovascular disease [21-25]. These benefits for the patients could be explained due to glucuronic action without potential risks of hypoglycemia, osmotic diuresis and natriuresis, resulting in plasma volume reduction [21, 25] as well as epigenetic and pleiotropic effects [26] relating to alleviating pathologies oxidative stress, advanced glycation end products (AGEs) signaling pathway, inflammation with consequence of vascular complicationsn and augmented cardiovascular risk being accordingly bettered by the primary action of EMPA [26].

Materials and methods

Ethical issues

The methodologies of the DN animal model of the studies were approved by the Institute of Animal Care and Use Committee at Kaohsiung Chang Gung Memorial Hospital (Affidavit of Approval of Animal Use Protocol No. 2020-092204).

Animals were housed in an Association for Assessment and Accreditation of Laboratory Animal Care International (AAALAC; Frederick, MD, USA)-approved animal facility in our hospital with controlled temperature and light cycles (24°C and 12/12 light cycle).

Using the N2a cells of in vitro studies

To test the impact of ADMSCs treatment on protecting the cells against the high concentration of glucose damage, the Neuro-2a cells (i.e., N2a cells) which are mouse neuroblasts were categorized into Group A1 [i.e., Neuro-2a cells (3.0×10^4 cells/12 wells to 1.0×10^6 cells/6 wells) cultured for 72 h in bottom of the Transwell], Group A2 [N2a cells + glucose (25 mM) co-cultured for 72 h in bottom of the Transwell], Group A3 [N2a cells + glucose (25 mM) co-cultured for 72 h in bottom of the Transwell, followed by adding ADMSCs ($1.x \times 10^4$ cells/12 wells to 5.0×10^5 cells/6 wells) in upper compartment of Transwell co-cultured for additional 72 h]. After cell culturing,

the N2a cells were obtained for individual analysis.

Besides, to elucidate the effect of empagliflozin treatment on protecting the cells against the high concentration of glucose damage, the N2a cells were categorized into Group B1 [N2a cells (1.0×10^6 cells/6 wells cultured for 72 h)], Group B2 [N2a cells + glucose (25 mM) co-cultured for 72 h], Group B3 [N2a cells + glucose (25 mM) co-cultured for 72 h, followed by adding EMPA (50 μM, i.e., defined as low dose) co-cultured for 48 h] and Group B4 [N2a cells + glucose (25 mM) co-cultured for 48 h, followed by adding EMPA (150 μM, i.e., defined as high dose) co-cultured for 48 h]. After cell culturing, the N2a cells were obtained for individual analysis. The dose of empagliflozin utilized for the in vitro study was based on our previous investigation [27].

DM induction for investigating DN in the current study (Referred to Supplementary Figure 1)

The methodologies of DM induction were conducted according to our previous study [28, 29]. Sprague-Dawley (SD) rats (n = 70) were utilized in th epresent study. In detail, streptozotocin (STZ/65 mg/kg) by intraperitoneal administration was conducted one time merely, resulting in a DM animal model.

Our previous study has proved that animal model of DN was successfully induced using this method [28, 29]. Accordingly, this validated animal model of DN was used in the current study and the animals were then calsified into group 1 [sham control (SC)], group 2 (DN), group 3 [DN + EMPA (20 mg/kg/day, daily orally by flexible feeding-needle for 6 weeks since day 7 after DM induction)], group 4 [DN + allogenic ADMSCs (1.2×10^6 cells by penile venous injection at time intervals of 1, 3, 5 weeks after DM induction)] and group 5 (DN + EMPA + allogenic ADMSCs), respectively. The animal grouping was performed just at the time point of DM induced, i.e., at day 7 after STZ therapy. The dose of the ADMSCs to be administered was according to our previous report [30, 31] with minimal modification. Additionally, the dosage of empagliflozin was also based on our previous study [27]. Using this method of DN, only two animals died by day 3 after STZ treatment, i.e., prior to animal grouping.

The methodologies for monitoring the circulatory level of blood sugar has been described by our previous studies [28, 29, 32]. Briefly, fasting (i.e., for 12 h) blood glucose level of each rat was examined at 8:00-9:00 a.m. using a blood glucose monitor at baseline prior to and by day 7, followed by every week after DM induction.

Preparation of allogenic ADMSCs for different points of treatment

The methodolofies for preparing the ADMSCs have been described in detail in our previous investigations [30, 31, 33]. Biefly, adipose tissue preparation for culturing the ADMSCs was conducted in additional 18 animals for those of groups 4 and 5 treatments. Adipose tissues around the epididymis were gentallyisolated just at the 14 days prior to different time points of treatment. After removing the fatty layer from the tube, the cell pellet was resuspended in 40 mL saline, followed by centrifugation again at 600 g for 5 min. Finally, the cell suspension was removed for cell culture in DMEM-low glucose medium containing 10% fetal bovine serum (FBS) for at least 14 days. Approximately $2.5\text{-}3.5 \times 10^6$ ADMSCs were obtained from each animal.

Behavioral assessment for mechanical paw withdrawal threshold (MPWT) and thermal paw withdrawal latency (TPWL) (Referred to Supplementary Figure 1)

The methodologies for mecahnical-sensory tests have been depicted in our previous study [11, 31]. In detail, to assess the impact of ADMSC-empagliflozin therapy on suppressing the DN after DM induction, the thermal and mechanical nociceptive thresholds were examined prior to DN induction and on days 1 (i.e., indicated the DM was successfully induced at 7^{th} day after STZ treatment), 7, 14, 28, 35 and 42 after DM induction, respectively.

To assess the thermal hyperalgesia, each animal was placed on a glass plate and radiant heat (Plantar Test Apparatus; Ugo Basile, Italy) was applied to the plantar surface of the surgical hind paw. The withdrawal latency and duration were annotated, with a minimum value set at 0.1 s and a cut-off latency set at 30 s to escape from the paw damage. Each animal was assessed for a total of three times at an inter-

val of 5 min, and the mean value was utilized in the following data analysis.

To evaluate the mechanical allodynia, each rat was put on the chamber and a servo-controlled mechanical stimulator (Dynamic Plantar Aesthesiometer; Ugo Basile, Italy) was exerted to the plantar surface of the operated hind paw repeatedly at 5-min intervals with gradually enhancing punctate pressure until the animal withdrew its paw. A maximal cut-off value was set at 50 g to prevent paw damage. The threshold was examined thrice for each time point and mean values were utilized for the following analysis.

Immunofluorescent (IF) staining

The methodologies of IF staining have been depicted in our previous investigations [11, 27, 29-33]. Briefly, rehydrated paraffin sections were first treated with 3% H_2O_2 for 30 minutes and incubated with Immuno-Block reagent (BioSB, Santa Barbara, CA, USA) for 30 minutes at room temperature. Sections were then incubated with primary antibodies specifically against phosphorylated (p)-p38 (1:200, Gene Tex), NF200 (1:200, Sigma-Aldrich), peripherin (1:1000, Abcam), 53BP1 (1:700, Novus) and β3 Tubulin (1:200, Santa Cruz). Sections were incubated with irrelevant antibodies served as controls. Three sections of dorsal root ganglia (DRG) specimens were analysed in each rat. For quantification, three randomly selected high-power fields (HPFs) were analysed per section. The mean number of positively stained cells per HPF for each group of the animals was derived across all nine HPFs.

Western blot analysis

The L4-L5 DRGs and the corresponding dorsal horn of the spinal cord from the rats of the sham control and experimental groups were harvested as previously described [11, 27, 30-33]. Equal amounts (50 μg) of protein extracts were loaded and separated by SDS-PAGE using 8-12% acrylamide gradients. After electrophoresis, the separated proteins were transferred electrophoretically to a polyvinylidene difluoride (PVDF) membrane (Amersham Biosciences). Nonspecific sites were blocked by incubation of the membrane in blocking buffer [5% nonfat dry milk in T-TBS (TBS containing 0.05% Tween 20)] overnight. The membranes were incubated with the indicated primary antibodies [NOX1 (1:1000, Sigma), NOX2 (1:1000, Sigma), γ-H2AX (1:1000, Cell Signaling), caspase3 (1:1000, Cell Signaling), poly (ADP-ribose) polymerase (PARP) (1:1000, Cell Signaling), mitochondrial Bax (1:1000, Abcam), Beclin-1 (1:1000, Cell Signaling), Atg5 (1:1000, Cell Signaling), LC3B (1:2000, Abcam), phosphorylated (P)-Smad3 (1:1000, Cell Signaling), transforming growth factor (TGF)-β (1:1000, Abcam), tumor necrosis factor (TNF)-α (1:1000, Cell Signaling), p-nuclear (NF)-κB (1:1000, Cell Signaling), Sirtuin 1 (SIRT1) (1:1000, Abcam), Nuclear factor erythroid 2-related factor 2 (Nrf2) (1:1000, Abcam), SIRT3 (1:500, Abcam), endothelial nitric oxide synthase (eNOS) (1:1000, Abcam), cytosolic cytochrome C (1:5000, BD), interleukin (IL-1β) (1:1000, Cell Signaling), glial fibrillary acidic protein (GFAP) (1:1000, Abcam), OX42 (1:1000, Abcam), p-P38 (1:1000, Sigma), phosphorylated c-Jun N-terminal kinase (p-JNK)1/2 (1:1000, Abcam), p-ERK1/2 (1:5000, Millipore), Nav1.3 (1:1000, Alomone), Nav1.8 (1:1000, Abcam), Nav1.9 (1:1000, Alomone), Actin (1:6000, Millipore) and VDAC1 (1:1000, Abcam)] for 1 hour at room temperature. Horseradish peroxidase-conjugated anti-rabbit immunoglobulin IgG (1:5000, Sigma) was used as the secondary antibody for 1 h incubation at room temperature. The washing procedure was repeated eight times within an hour, and immunoreactive bands were visualized by enhanced chemiluminescence (ECL; Amersham Biosciences) after exposure to Biomax L film (Kodak). For quantification, ECL signals were digitized using Labwork software (UVP).

Statistical analysis

Quantitative data are expressed as mean ± SD. Statistical analysis was performed by ANOVA followed by Bonferroni multiple comparison post-hoc test. SAS statistical software for Windows version 8.2 (SAS Institute, Cary, NC, USA) was utilized. A probability value <0.05 was considered statistically significant.

Results

*ADMSCs treatment reversed hyperglycemia enhanced β-galactosidase and γ-H2AX positively stained expression in N2a cells (**Figure 1**)*

To elucidate whether the ADMSCs would alleviate the hyperglycemia-induced cellular levels of

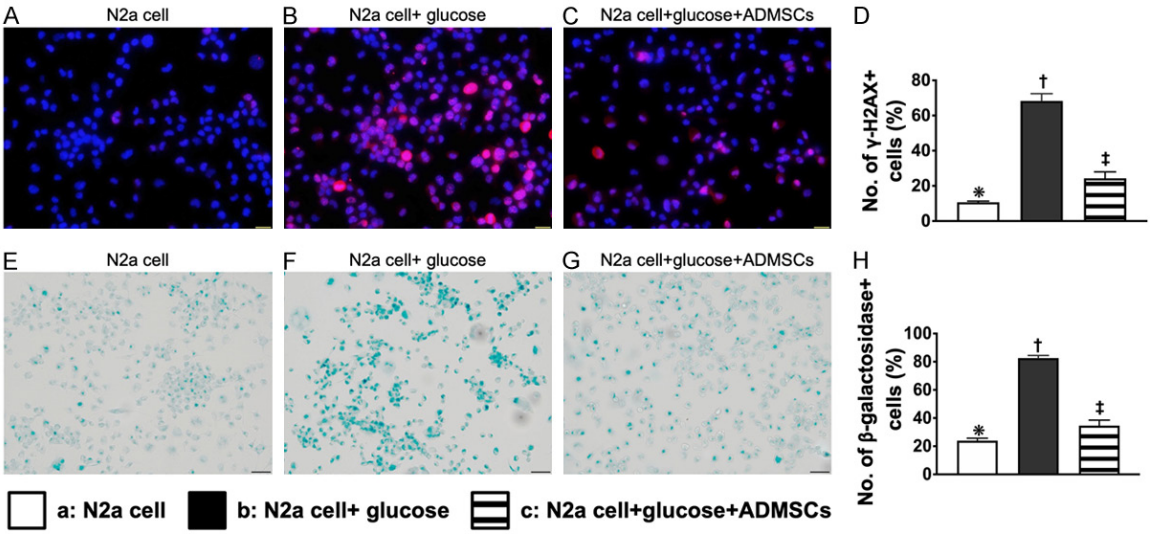

Figure 1. ADMSCs treatment suppressed hyperglycemic induced β-galactosidase and γ-H2AX positively stained in N2a cells. A-C. Illustrating the immunofluorescent (IF) microscopic finding (400×) for identification of γ-H2AX+ cells (pink color). Scale bars in lower right corner represent 20 μm. D. Analytical result of number of positively stained γ-H2AX cells, * vs. other groups with different symbols (†, ‡), P<0.001. E-G. Illustrating the immunohistochemical microscopic finding (200×) for identification of β-galactosidase + cells (green color). Scale bars in lower right corner represent 50 μm. H. Analytical result of number of positively stained β-galactosidase cells, * vs. other groups with different symbols (†, ‡), P<0.001. All statistical analyses were performed by one-way ANOVA, followed by Bonferroni multiple comparison post hoc test (n = 3 for each group). ADMSCs = adipose-derived mesenchymal stem cells. Symbols (*, †, ‡) indicate significance for each other (at 0.05 level). A1 = N2a cells; A2 = N2a cells + glucose; A3 = N2a cells + glucose + ADMSCs.

senescence and DNA damage, the IHC and IF stains for N2a cells were utilized in the present study. The result demonstrated that the number of N2a cells with positively stained β-galactosidase, an indicator of senescence, and positively stained γ-H2AX, an indicator of DNA damage, were significantly increased in Group A2 [N2a cells + glucose (25 mM)] than in Group A1 (N2a cells) that were significantly reversed in Group A3 [N2a cells + glucose (25 mM) + ADMSCs].

*ADMSCs treatment reversed hyperglycemia reduced the cellular expression of mitochondrial cytochrome C and the protein levels of oxidative stress in N2a cells (**Figure 2**)*

Next, we wanted to investigate whether ADMSCs could ameliorate the hyperglycemia enhanced mitochondrial damage and oxidative stress. IF microscope and Western blot were utilized for our purposes in cellular groups A1, A2 and A3, as shown in **Figure 1**. As we expected, the cellular level of mitochondrial cytochrome C, an indicator of mitochondrial integrity, was significantly lower in Group A2 than in Group A1 that was significantly reversed in Group A3. Additionally, the protein expressions of NOX-1, NOX-2 and oxidized protein, three indicators of oxidative stress, displayed an opposite pattern of mitochondrial cytochrome C among the groups.

*ADMSCs treatment reversed hyperglycemia induced apoptosis, DNA damage and autophagy in N2a cells (**Figure 3**)*

Further, based on the cell grouping A1, A2 and A3, as shown in **Figure 1**, we decided to assess whether ADMSCs treatment could reduce hyperglycemia induced molecular perturbations in N2a cells. Western blot analysis was applied in the in vitro study. The result demonstrated that the protein expressions of cleaved caspase 3 and cleaved PARP, two indices of apoptosis, protein expression of γ-H2AX, one indicator of DNA-damaged marker, and protein expression of Agt5, beclin-1 and ratio of LC3B-II to LC3B-I, three indices of autophagy, were significantly higher in A2 than in A1 and A3, and significantly higher in A3 than in A1.

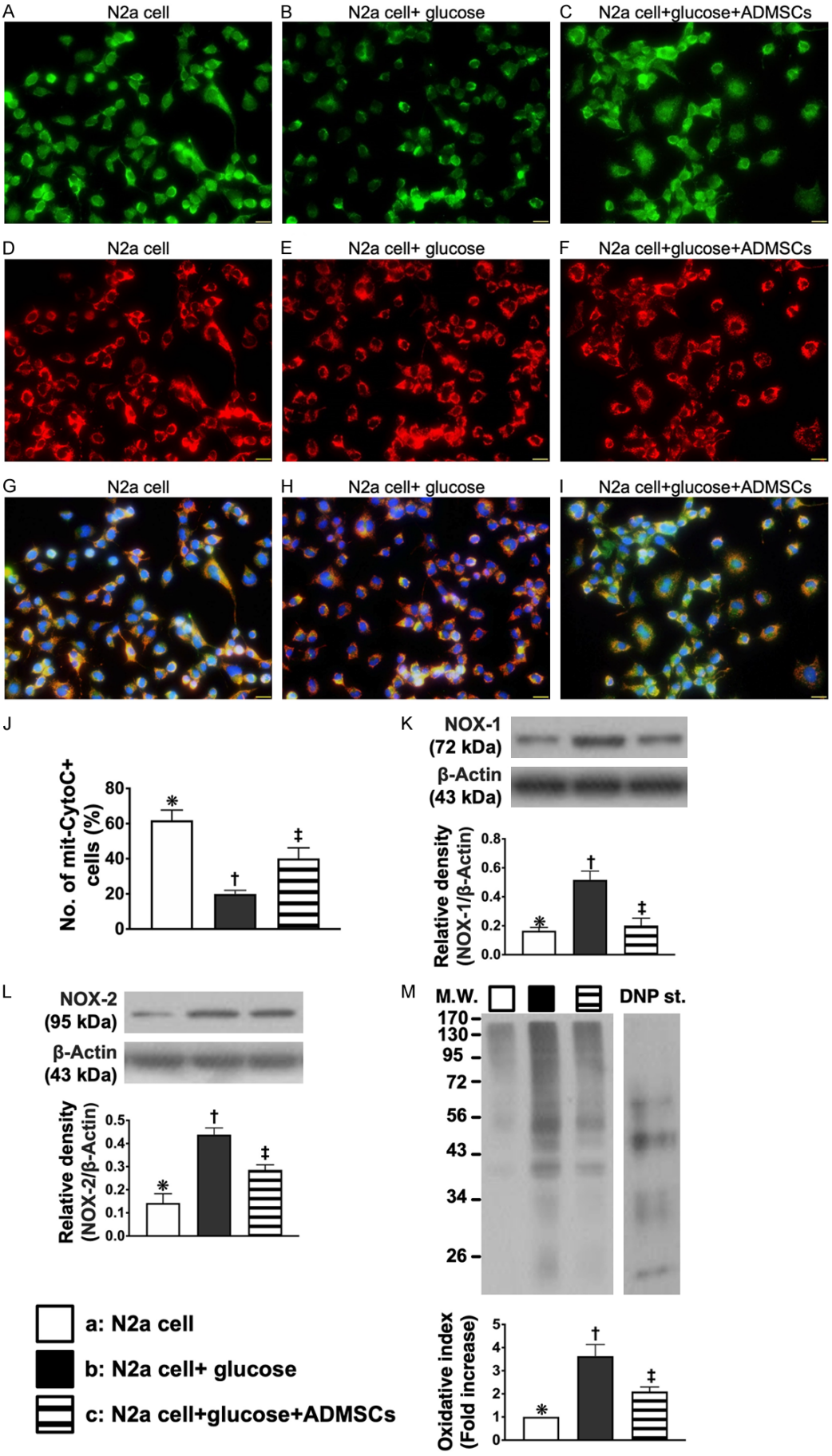
A
N2a cell
B
N2a cell+ glucose
C
N2a cell+glucose+ADMSCs
D
N2a cell
E
N2a cell+ glucose
F
N2a cell+glucose+ADMSCs
G
N2a cell
H
N2a cell+ glucose
I
N2a cell+glucose+ADMSCs
J
No. of mit-CytoC+ cells (%)
K
NOX-1 (72 kDa)
β-Actin (43 kDa)
Relative density (NOX-1/β-Actin)
L
NOX-2 (95 kDa)
β-Actin (43 kDa)
Relative density (NOX-2/β-Actin)
M
M.W.
DNP st.
170
130
95
72
56
43
34
26
Oxidative index (Fold increase)
a: N2a cell
b: N2a cell+ glucose
c: N2a cell+glucose+ADMSCs

Figure 2. ADMSC treatment reversed hyperglycemia reduction of the cellular expression of mitochondrial cytochrome C and enhanced the protein levels of oxidative stress in N2a cells. A-C. Illustrates the immunofluorescent (IF) microscopic finding (400×) for identification of mitochondrial cytochrome C+ cells (green color) in N2a cells. D-F. Illustrates IF microscopic finding (400×) for identification of heat shock protein 60 (HSP60)+ cells (red color) in N2a cells. G-I. Illustrates IF microscopic finding (400×) of merged cytochrome C and HSP60 positively stained cells (i.e., double stain) for identification of cytochrome C in mitochondria (i.e., pink color). Blue color indicated nuclei stained by DAPI. J. Analytical result of number of mitochondrial cytochrome C (No. of mit-CytoC)+ cells in N2a cells, * vs. other group with different symbols (†, ‡), P<0.001. Scale bars in right lower corner represent 20 μm. K. Protein expression of NOX-1, * vs. other group with different symbols (†, ‡), P<0.001. L. Protein expression of NOX-2, * vs. other group with different symbols (†, ‡), P<0.001. M. The oxidized protein expression, * vs. other groups with different symbols (†, ‡), P<0.001 (Note: the left and right lanes shown on the upper panel represent protein molecular weight marker and control oxidized molecular protein standard, respectively). M.W. = molecular weight; DNP = 1-3 dinitrophenylhydrazone. All statistical analyses were performed by one-way ANOVA, followed by Bonferroni multiple comparison post hoc test (n = 3 for each group). Symbols (*, †, ‡) indicate significance for each other (at 0.05 level). ADMSCs = adipose-derived mesenchymal stem cells. A1 = N2a cells; A2 = N2a cells + glucose; A3 = N2a cells + glucose + ADMSCs.

*ADMSCs treatment suppressed hyperglycemia induced inflammation and preserved intrinsic capacity of anti-oxidant in N2a cells (**Figure 4**)*

Based on the cell grouping A1, A2 and A3, as shown in **Figure 1**, we utilized Western blot analysis again to examine the molecular levels of inflammatory and anti-oxidant biomarkers. The result demonstrated that the protein expressions of NF-κB and TNF-α, two indicators of inflammation, were significantly increased in A2 than in A1 and A3 and significantly increased in A3 than in A1. On the hand, the protein expressions of Nrf2, SIRT1, SIRT3 and eNOS, four indicators of anti-oxidants, displayed an opposite manner of inflammation among the groups.

*EMPA treatment reversed hyperglycemia induced oxidative stress and autophagy in N2a cells (**Figure 5**)*

To investigate the molecular levels of oxidative stress and autophagy, the Na2 cells were categorized into group B1 (N2a cells), group B2 [N2a cells + glucose (25 mM)], group B3 [N2a cells + glucose (25 mM) + EMPA (50 μM)] and group B4 [N2a cells + glucose (25 mM) + EMPA (150 μM)], respectively. The result showed that the protein expression of NOX-1, NOX-2 and oxidized protein, three indices of oxidative stress, and protein expressions of Atg5, beclin-1 and ratio of LC3B-II to LC3B-I, three indices of autophagy, were lowest in B1 and significantly and progressively reduced from B2 to B4.

*EMPA treatment reversed hyperglycemia induced apoptosis, fibrosis and DNA damage in N2a cells (**Figure 6**)*

Based on the cellular grouping of **Figure 5**, we desired to explore whether empagliflozin treatment could attenuate hyperglycemia induced molecular perturbations of apoptosis, fibrosis and DNA damage in the culturing N2a cells. The result showed that the protein expressions of mitochondrial Bax, cleaved caspase 3 and cleaved PARP, three indicators of apoptosis, protein expressions of Smad3 and TGF-β, two biomarkers of fibrosis, and protein expression of γ-H2AX, an indicator of DNA damage, were lowest in B1 and significantly and progressively reduced from B2 to B4.

*Serial changes of blood sugar and body weight (BW) among the five groups of the animals (**Table 1**)*

Based on the findings of the *in vitro* study, we suggested that ADMSCs-EMPA therapy could offer additional benefits on protecting the nervous system from hyperglycemia damage. Accordingly, we derived a DM animal model, defined as hyperglycemic diabetic neuropathy (DN). First, we regularly measured the circulatory level of blood sugar. The result demonstrated that the baseline blood sugar did not differ among the groups 1 (SC), 2 (DN), 3 (DN + EMPA), 4 (DN + allogenic ADMSCs) and 5 (DN + EMPA + allogenic ADMSCs). However, by 7th day (defined as day 1 after successful DM induction) after STZ treatment, the blood sugar was significantly higher in groups 2 to 5 than in group 1, but it showed no difference among the groups 2 to 5. However, by days 7, 14, 21, 28, 35 and 42 after DM induction, this parameter was significantly higher in groups 2 and 4 than in groups 1, 3 and 5 but it was similar among the groups 1, 3 and 5. Additionally, by days 7, 14 and 21 after DM induction, this parameter was similar between groups 2 and 4, whereas by days 28, 35 and 42, this parameter was significantly lower in group 4 than in group 2. The

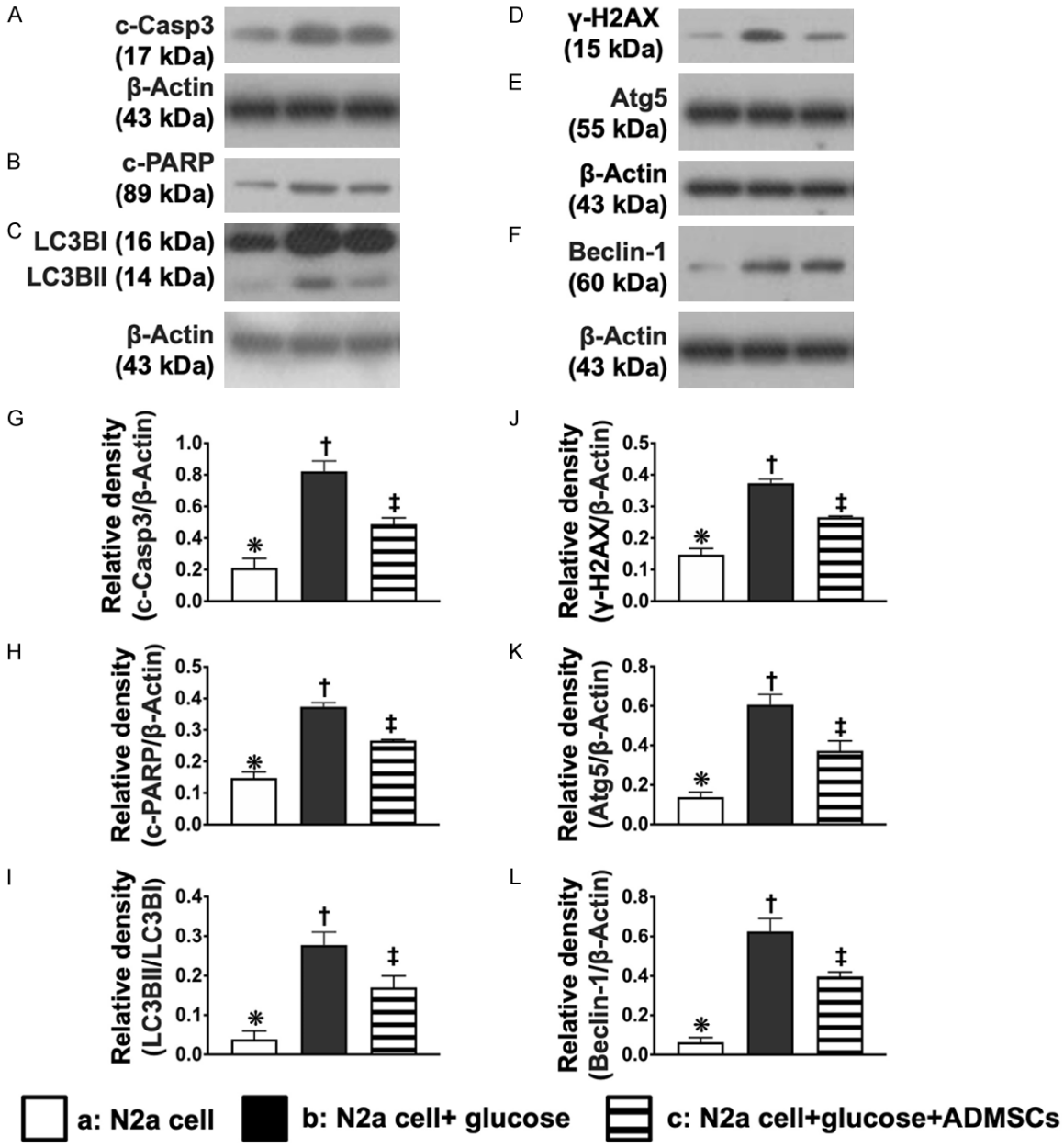

Figure 3. ADMSC treatment alleviated hyperglycemia-induced apoptosis, DNA damage and autophagy in N2a cells. A and G. Protein expression of cleaved caspase 3 (c-Casp3), * vs. other groups with different symbols (†, ‡), P<0.001. B and H. Protein expression of cleaved poly(ADP-ribose) polymerase (c-PARP), * vs. other groups with different symbols (†, ‡), P<0.001. C and I. Protein expression of ratio of LC3B-II to LC3B-I, * vs. other groups with different symbols (†, ‡), P<0.001. D and J. Protein expression of γ-H2AX, * vs. other groups with different symbols (†, ‡), P<0.001. E and K. Protein expression of Agt5, * vs. other groups with different symbols (†, ‡), P<0.001. F and L. Protein expression of beclin-1, * vs. other groups with different symbols (†, ‡), P<0.001. All statistical analyses were performed by one-way ANOVA, followed by Bonferroni multiple comparison post hoc test (n = 3 for each group). Symbols (*, †, ‡) indicate significance for each other (at 0.05 level). ADMSCs = adipose-derived mesenchymal stem cells. A1 = N2a cells; A2 = N2a cells + glucose; A3 = N2a cells + glucose + ADMSCs.

findings of groups 1, 3 and 5 implicated that EMPA treatment immensely effectively controlled the circulatory hyperglycemia. Additionally, the result from groups 4 and 2 implicated that the much lower hyperglycemia in the former than in the latter group could be

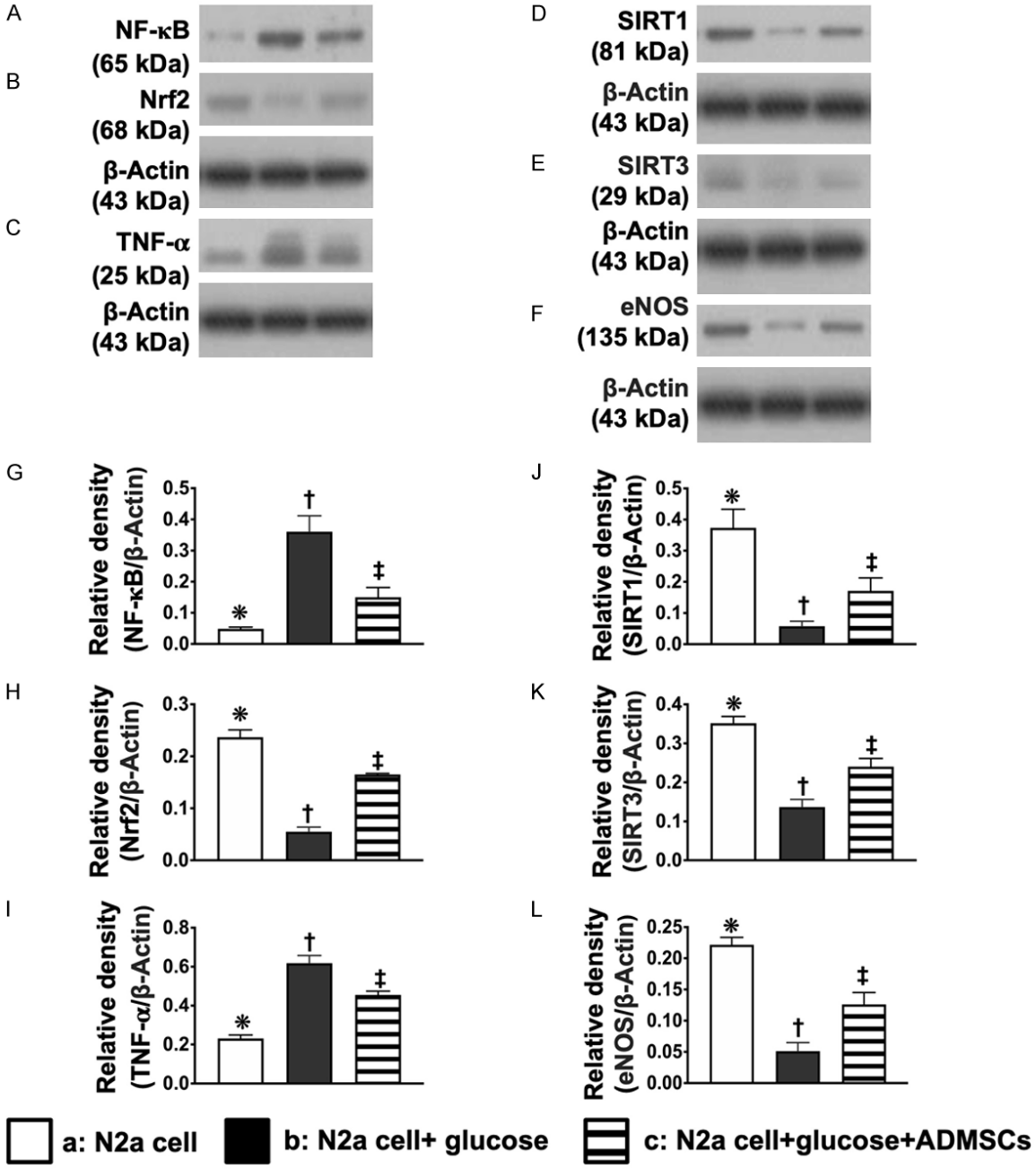

Figure 4. ADMSC treatment suppressed hyperglycemia-induced inflammation and preserved intrinsic capacity of anti-oxidant in N2a cells. A and G. Protein expression of nuclear factor (NF)-κB, * vs. other groups with different symbols (†, ‡), P<0.001. B and H. Protein expression of Nrf2, * vs. other groups with different symbols (†, ‡), P<0.001. C and I. Protein expression of tumor necrosis factor (TNF)-α, * vs. other groups with different symbols (†, ‡), P<0.001. D and J. Protein expression of SIRT1, * vs. other groups with different symbols (†, ‡), P<0.001. E and K. Protein expression of SIRT3, * vs. other groups with different symbols (†, ‡), P<0.001. F and L. Protein expression of endothelial nitric oxide synthase (eNOS), * vs. other groups with different symbols (†, ‡), P<0.001. All statistical analyses were performed by one-way ANOVA, followed by Bonferroni multiple comparison post hoc test (n = 3 for each group). Symbols (*, †, ‡) indicate significance for each other (at 0.05 level). ADMSCs = adipose-derived mesenchymal stem cells. A1 = N2a cells; A2 = N2a cells + glucose; A3 = N2a cells + glucose + ADMSCs.

explained as the effect of ADMSCs on partially protecting the β-cell in pancreas against the STZ destruction.

When we looked at the time courses of the rat BW, we found that the baseline and at the time point of day 1 after DM was successfully

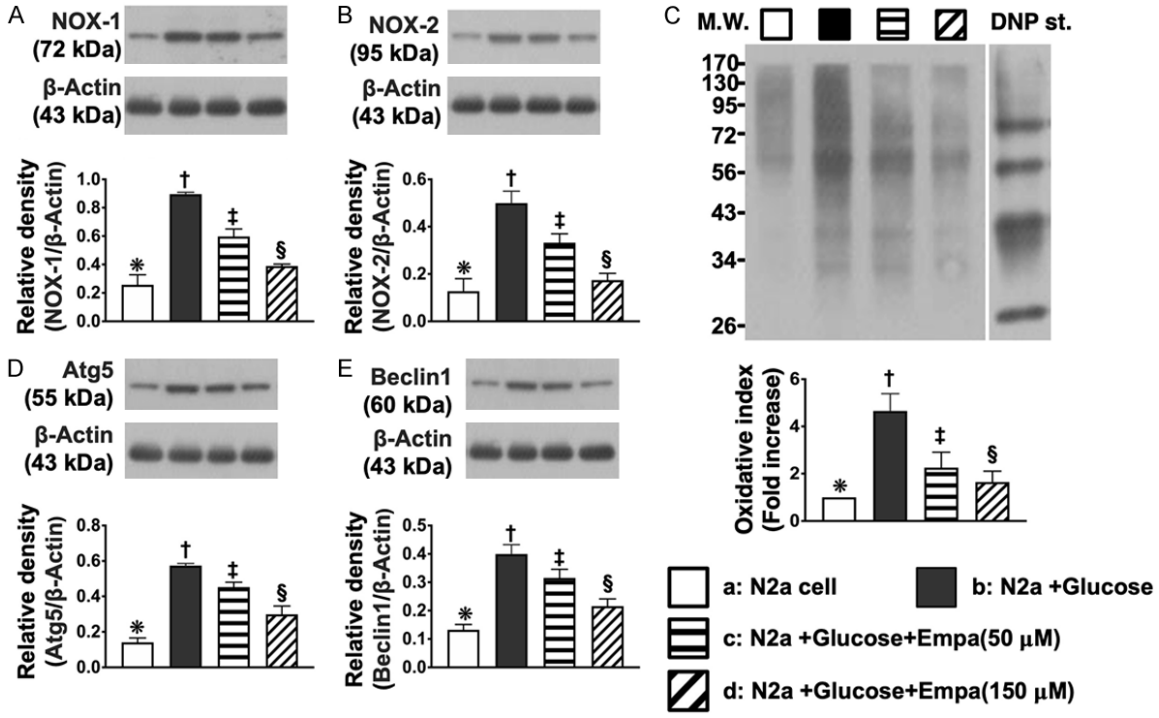

Figure 5. Empagliflozin treatment reversed hyperglycemia induced oxidative stress and autophagy in N2a cells. A. Protein expression of NOX-1, * vs. other groups with different symbols (†, ‡, §), P<0.001. B. Protein expression of NOX-2, * vs. other groups with different symbols (†, ‡, §), P<0.001. C. The oxidized protein expression, * vs. other groups with different symbols (†, ‡, §), P<0.001 (Note: the left and right lanes shown on the upper panel represent protein molecular weight marker and control oxidized molecular protein standard, respectively). M.W. = molecular weight; DNP = 1-3 dinitrophenylhydrazone. D. Protein expression of Atg5, * vs. other groups with different symbols (†, ‡, §), P<0.001. E. Protein expression of Beclin 1, * vs. other groups with different symbols (†, ‡, §), P<0.001. All statistical analyses were performed by one-way ANOVA, followed by Bonferroni multiple comparison post hoc test (n = 3 for each group). Symbols (*, †, ‡, §) indicate significance for each other (at 0.05 level). B1 = N2a cells; B2 = N2a cells + glucose; B3 = N2a cells + glucose + Empa (50 μM); B4 = N2a cells + glucose + Empa (150 μM). Empa = empagliflozin.

induced, the BW was similar among the five groups. Additionally, the BW in group 1 was significantly and progressively increased from day 1 to day 42 after successfully DM induction, whereas the BW in groups 2 and 5 was significantly and progressively reduced with respect to these time intervals. However, at the end of the study period, the BW was significantly lower in group 2 than in groups 3 to 5 whereas it showed no difference among these latter three groups. This finding implicated that EMPA that could maintain the normal blood sugar might have ability of reducing BW in groups 3 and 5 of rodent. Additionally, the reduction of BW being notably less severe in group 4 than in group 2 once again indirectly confirmed that ADMSCs treatment would partially safeguard the β-cell in pancreas far away from the STZ damage.

*Time courses of TPWL (sec) and MPWT (g) in rats (**Figure 7**)*

Next, when we looked at the animal behavioral tests, i.e., the serial changes of MPWT and TPWL that are the principal tests for verifying the degree of DN, we found that prior to successful DM induction (i.e., verified as a marked increase of hyperglycemia in each animal by day 7 after STZ therapy), both MPWT and TPWL did not differ among the groups 1 to 5. Additionally, MPWT and TPWL did not differ among the time intervals of days 1, 7, 14, 21, 28, 35 and 42 after successfully DM induction in group 1. However, as compared with group 1, these two parameters were significantly upregulated in group 2 at these time intervals that was significantly reversed in group 4, further significantly reversed in group 3, and furthermore significantly reversed in group 5. Our find-

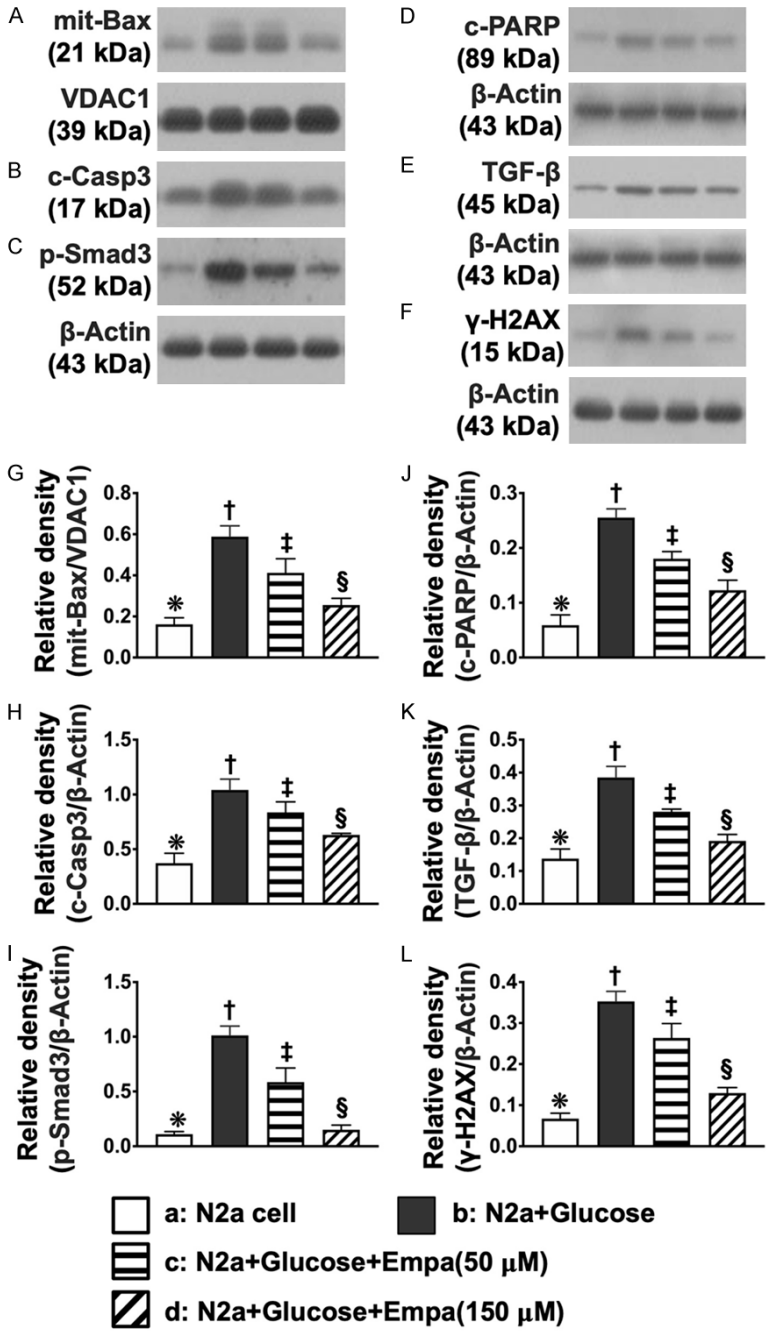

Figure 6. Empagliflozin treatment reversed hyperglycemia induced apoptosis, fibrosis and DNA damage in N2a cells. A and G. Protein expression of mitochondrial (mit)-Bax, * vs. other groups with different symbols (†, ‡, §), P<0.001. B and H. Protein expression of cleaved caspase 3 (c-Casp3), * vs. other groups with different symbols (†, ‡, §), P<0.001. C and I. Protein expression of phosphorylated (p)-Smad3, * vs. other groups with different symbols (†, ‡, §), P<0.001. D and J. Protein expression of Protein expression of cleaved poly(ADP-ribose) polymerase (c-PARP), * vs. other groups with different symbols (†, ‡, §), P<0.001. E and K. Protein expression of transforming growth factor (TGF)-β, * vs. other groups with different symbols (†, ‡, §), P<0.001. F and L. Protein expression of γ-H2AX, * vs. other groups with different symbols (†, ‡, §), P<0.001. All statistical analyses were performed by one-way ANOVA, followed by Bonferroni multiple comparison post hoc test (n = 3 for each group). Symbols (*, †, ‡, §) indicate significance for each other (at 0.05 level). B1 = N2a cells; B2 = N2a cells + glucose; B3 = N2a cells + glucose + Empa (50 μM); B4 = N2a cells + glucose + Empa (150 μM). Empa = empagliflozin.

ings showed that pain sensitivity was markedly impaired in DN animals. Additionally, the therapeutic effect of combined ADMSCs + EMPA was superior to one therapy alone in protecting the neurons/nerves against the DN injury.

*Impact of ADMSCs-EMPA therapy on suppressing the protein expressions of oxidative stress and apoptosis in L4-L5 levels of DRGs by day 42 after successful DM induction (**Figure 8**)*

By using the specimen from L4-L5 levels of DRGs, we analyzed the protein expressions of NOX-1, NOX-2 and oxidized protein, three indicators of oxidative stress, and the protein expressions of mitochondrial-Bax, cleaved caspase 3 and cleaved PARP, three indices of apoptosis, were lowest in group 1, highest in group 2, significantly lower in group 5 than in groups 3 and 4 and significantly lower in group 3 than in group 4, suggesting that combined ADMSCs and EMPA was superior to merely one therapy for protecting the nervous system against hyperglycemic damage.

*Impact of ADMSCs-EMPA therapy on suppressing the protein expressions of fibrosis, mitochondrial/DNA damage and inflammation in L4-L5 levels of DRGs by day 42 after successful DM induction (**Figure 9**)*

Next, we utilized western blot to assess the protein expressions of Smad3 and TGF-β, two fibrotic biomarkers, protein expressions of GFAP, IL-1β and OX-42, three indices of inflammatory reaction and protein expression of γ-H2AX, a DNA-damaged markers as well as the protein expression

Table 1. Serial changes of blood sugar and body weight in five groups

Variables	Baseline*	D1†	D7	D14	D21	D28	D35	D42	$P^{D1 \text{ vs. } D42}$
BS (mg/dL)									
Group 1	77.7	84.8[a]	81.0[a]	89.2[a]	91.5[a]	99.5[a]	97.3[a]	92.1[a]	0.220
Group 2	78.3	505.9[b]	509.9[b]	526.7[b]	532.1[b]	559.2[b]	571.8[b]	598.8[b]	0.403
Group 3	78.1	496.9[b]	98.1[a]	100.7[a]	108.6[a]	116.5[a]	110.9[a]	106.1[a]	<.0001
Group 4	78.3	493.6[b]	412.0[b]	430.6[b]	466.8[b]	466.8[c]	469.3[c]	471.2[c]	0.441
Group 5	77.3	486.5[b]	89.1[a]	93.8[a]	99.1[a]	99.1[a]	106.9[a]	103.8[a]	<.0001
P-value	0.998	<.0001	<.0001	<.0001	<.0001	<.0001	<.0001	<.0001	
BW (g)									
Group 1	NA	353.4	370.5[a]	382.7[a]	405.6[a]	424.5[a]	433.9[a]	449.4[a]	<.0001
Group 2	NA	345.5	340.4[b]	325.0[b]	309.1[b]	295.4[b]	272.1[b]	252.9[b]	<.0001
Group 3	NA	348.8	338.6[b]	327.9[b]	322.6[b]	316.9[b]	303.8[b]	292.5[c]	<.0001
Group 4	NA	329.3	328.3[b]	319.6[b]	325.8[b]	320.6[b]	370.6[b]	300.3[c]	0.033
Group 5	NA	334.3	333.2[b]	328.8[b]	333.8[b]	326.7[b]	314.0[b]	309.2[c]	0.002
P-value	NA	0.077	0.001	<.0001	<.0001	<.0001	<.0001	<.0001	

*indicated healthy animals prior to streptozotocin treatment. †indicated by 7th day after streptozotocin treatment, i.e., defined as successfully induction of diabetes mellitus (DM). [a,b,c]denoted significant difference in BS or BW among groups at the same time point. *P*-value$^{D1 \text{ vs. } D42}$ in column was calculated with paired t test after comparison of values between days 1 and 42. Additionally, *P*-value in rows was calculated among five groups with one-way ANOVA followed by Bonferroni post hoc analysis for comparing the difference between two groups (n = 12-14 for each group). D = day; BS = blood sugar; group 1 = sham control (SC); group 2 = diabetic neuropathy (DN); group 3 = DN + empagliflozin (EMPA); group 4 = DN + adipose tissue-derived mesenchymal stem cells (ADMSCs); group 5 = DN + EMPA + ADMSCs.

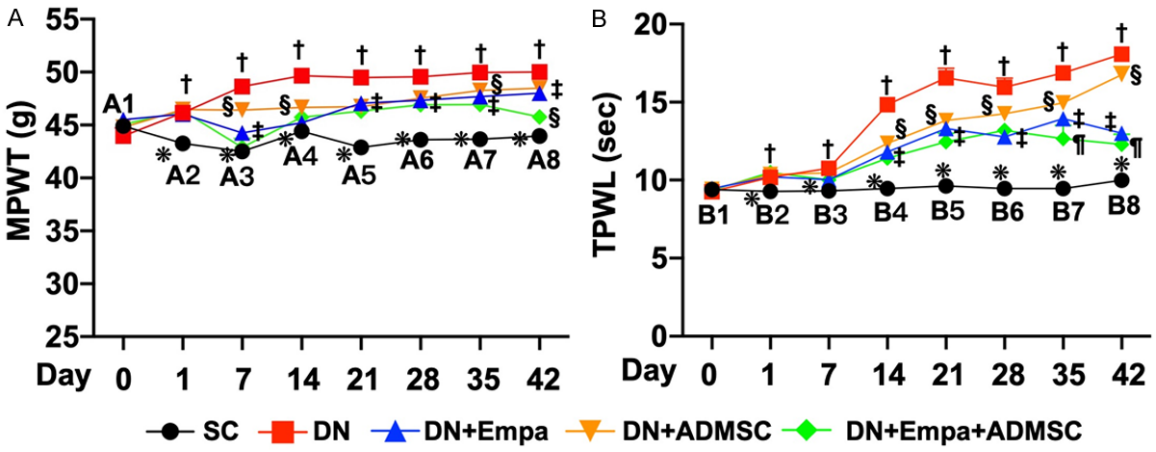

Figure 7. Time courses of MPWT (g) and TPWL (Sec) in rat. A: (A1) At baseline, the analytical result of MPWT was similar among the five groups. (A2) At day 1 after successful DM induction, the analytical result of MPWT, * vs. †, P<0.01. (A3) At day 7, the analytical results of MPWT, * vs. other groups with different symbols (†, ‡, §), P<0.001. (A4) At day 14, the analytical results of MPWT, * vs. other groups with different symbols (†, §), P<0.001. (A5) At day 21, the analytical results of MPWT, * vs. other groups with different symbols (†, ‡), P<0.001. (A6) At day 28, the analytical results of MPWT, * vs. other groups with different symbols (†, ‡), P<0.001. (A7) At day 35, the analytical results of MPWT, * vs. other groups with different symbols (†, ‡, §), P<0.0001. (A8) At day 42, the analytical results of MPWT, * vs. other groups with different symbols (†, ‡, §), P<0.0001. B: (B1) At baseline, the analytical results of TPWL were similar among the five groups. (B2) At day 1 after successful DM induction, the analytical results of TPWL, * vs. †, P<0.01. (B3) At day 7, the analytical results of TPWL, * vs. †, P<0.01. (B4) At day 14, the analytical results of TPWL, * vs. other groups with different symbols (†, ‡, §), P<0.001. (B5) At day 21, the analytical results of TPWL, * vs. other groups with different symbols (†, ‡, §), P<0.0001. (B6) At day 28, the analytical results of TPWL, * vs. other groups with different symbols (†, ‡, §), P<0.0001. (B7) At day 35, the analytical results of TPWL, * vs. other groups with different symbols (†, ‡, §, ¶), P<0.0001. (B8) At day 42, the analytical results of TPWL, * vs. other groups with different symbols (†, ‡, §, ¶), P<0.0001. All statistical analyses were performed by one-way ANOVA, followed by Bonferroni multiple comparison post hoc test (n = 12-14 for each group). Symbols (*, †, ‡, §, ¶) indicate significance for each other (at 0.05 level). Group 1 = sham-control (SC); group 2 = diabetic neuropathy (DN); group 3 = DN + Empa; group 4 = DN + allogenic ADMSCs; group 5 = DN + Empa + allogenic ADMSCs; DM = diabetes mellitus; Empa = empagliflozin; TPWL = thermal paw withdrawal latency; MPWT = mechanical paw withdrawal threshold.

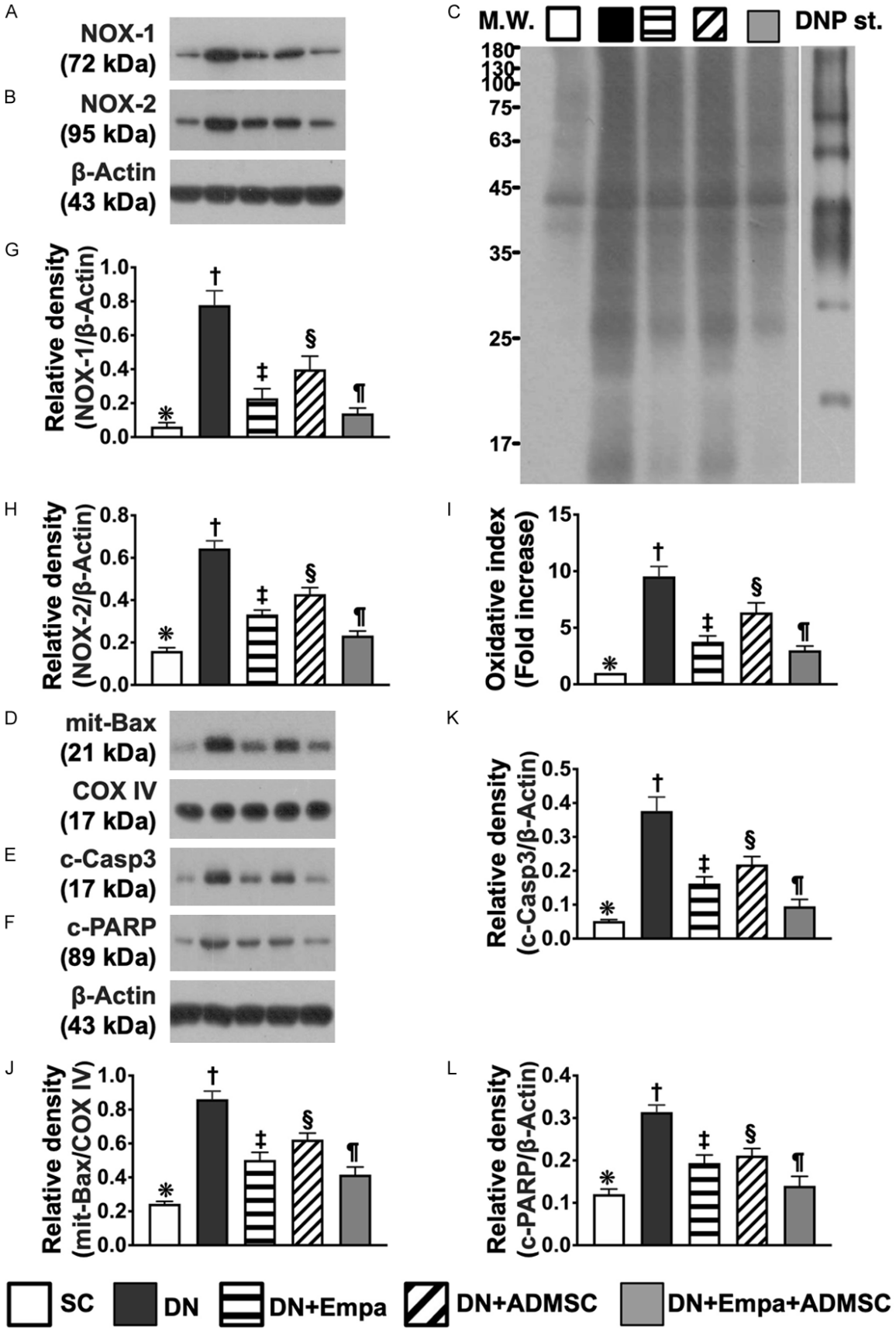
A
NOX-1
(72 kDa)
B
NOX-2
(95 kDa)
β-Actin
(43 kDa)
C
M.W.
DNP st.
180
130
100
75
63
45
35
25
17
G
Relative density
(NOX-1/β-Actin)
H
Relative density
(NOX-2/β-Actin)
I
Oxidative index
(Fold increase)
D
mit-Bax
(21 kDa)
COX IV
(17 kDa)
E
c-Casp3
(17 kDa)
F
c-PARP
(89 kDa)
β-Actin
(43 kDa)
K
Relative density
(c-Casp3/β-Actin)
J
Relative density
(mit-Bax/COX IV)
L
Relative density
(c-PARP/β-Actin)
SC
DN
DN+Empa
DN+ADMSC
DN+Empa+ADMSC

Figure 8. Effect of ADMSCs-empagliflozin therapy on suppressing the protein expressions of oxidative stress and apoptosis by day 42 after successful DM induction. A and G. Protein expression of NOX-1, * vs. other groups with different symbols (†, ‡, §, ¶), P<0.0001. B and H. Protein expression of NOX-2, * vs. other groups with different symbols (†, ‡, §, ¶), P<0.0001. C and I. The oxidized protein expression, * vs. other groups with different symbols (†, ‡, §, ¶), P<0.0001 (Note: the left and right lanes shown on the upper panel represent protein molecular weight marker and control oxidized molecular protein standard, respectively). M.W. = molecular weight; DNP = 1-3 dinitrophenylhydrazone. D and J. Protein expression of mitochondrial (mit)-Bax, * vs. other groups with different symbols (†, ‡, §, ¶), P<0.0001. E and K. Protein expression of cleaved caspase 3 (c-Casp3), * vs. other groups with different symbols (†, ‡, §, ¶), P<0.0001. F and L. Protein expression of cleaved poly (ADP-ribose) polymerase (c-PARP), * vs. other groups with different symbols (†, ‡, §, ¶), P<0.0001. All statistical analyses were performed by one-way ANOVA, followed by Bonferroni multiple comparison post hoc test (n = 6 for each group). Symbols (*, †, ‡, §, ¶) indicate significance for each other (at 0.05 level). Group 1 = sham-control (SC); group 2 = diabetic neuropathy (DN); group 3 = DN + Empa; group 4 = DN + allogenic ADMSCs; group 5 = DN + Empa + allogenic ADMSCs. ADMSCs = adipose-derived mesenchymal stem cells; Empa = empagliflozin.

of cytosolic cytochrome C, an index of mitochondrial damage, were lowest in group 1, highest in group 2, significantly lower in group 5 than in groups 3 and 4 and significantly lower in group 3 than in group 4, whereas the protein expression of mitochondrial cytochrome C, an index of mitochondrial integrity, exhibited an opposite pattern of cytosolic cytochrome C among the groups.

*Impact of ADMSCs-EMPA therapy on suppressing the protein expressions of autophagy and pain-facilitated biomarkers in L4-L5 levels of DRGs by day 42 after successful DM induction (**Figure 10**)*

To elucidate whether ADMSCs-EMPA therapy could effectively ameliorate the autophagic and pain-facilitated biomarkers in L4-L5 levels of DRGs, western blot analysis was utilized once again in the present study. The results demonstrated that the protein expressions of Atg5, beclin-1 and the ratio of LC3B-II to LC3B-I, three indices of autophagy, protein expressions of MAPK family members (p-P38, p-JNK, p-ERK1/2), three pain-facilitated biomarkers, and protein expressions of voltage-gated sodium channels (Nav.1.3, Nav.1.8, Nav.1.9) served as the pain signalings [34], were lowest in group 1, highest in group 2, significantly lower in group 5 than in groups 3 and 4 and significantly lower in group 3 than in group 4.

*Impact of ADMSCs-EMPA therapy on regulating the co-localization of p-P38-peripherin and p-P38-NF200 in L4-L5 levels of DRG neurons by day 42 after successful DM induction (**Figures 11, 12**)*

It is well recognized that peripherin which is small unmyelinated C-fiber and thinly myelinated A-δ fiber of DRG neurons conducts the thermal and noxious stimuli [11, 12]. Based on this issue above-mentioned [11, 12], we utilized the IF microscope to identify that the co-localization of p-P38 and peripherin (**Figure 11**) and the co-localization of p-P38 and NF200 (**Figure 12**) in DRG neurons were highest in group 2, lowest in group 1, significantly higher in group 4 than in groups 3 and 5, and significantly higher in group 3 than in group 5.

*Impact of ADMSCs-EMPA therapy on suppressing cellular expression of DNA damage in L4-L5 levels of DRGs by day 42 after successful DM induction (**Figure 13**)*

Finally, the IF microscope identified that the cellular expression of γ-H2AX in L4-L5 levels of DRGs, an index of DNA damage, was highest in group 2, lowest in group 1 and significantly progressively reduced from groups 3 to 5.

Discussion

This study which explored the therapeutic effects of ADMSCs-EMPA, delivered several preclinical implications. First, we successfully created a hyperglycemic neurological model that not only provided a useful tool for scientific research but also verified that persistence of hyperglycemia (i.e., DM) could really induce DN setting with clinical presentation of partially dysesthesia (i.e., marked loss of pain sensations). Second, in vitro and in vivo studies identically demonstrated that hyperglycemia elicited molecular-cellular perturbations that destroyed the neurons and nervous system. Third, the research further demonstrated that ADMSCs and EMPA effectively and combined ADMSCs and EMPA further effectively, reversed the dysesthesia, i.e., sluggish withdrawal of the

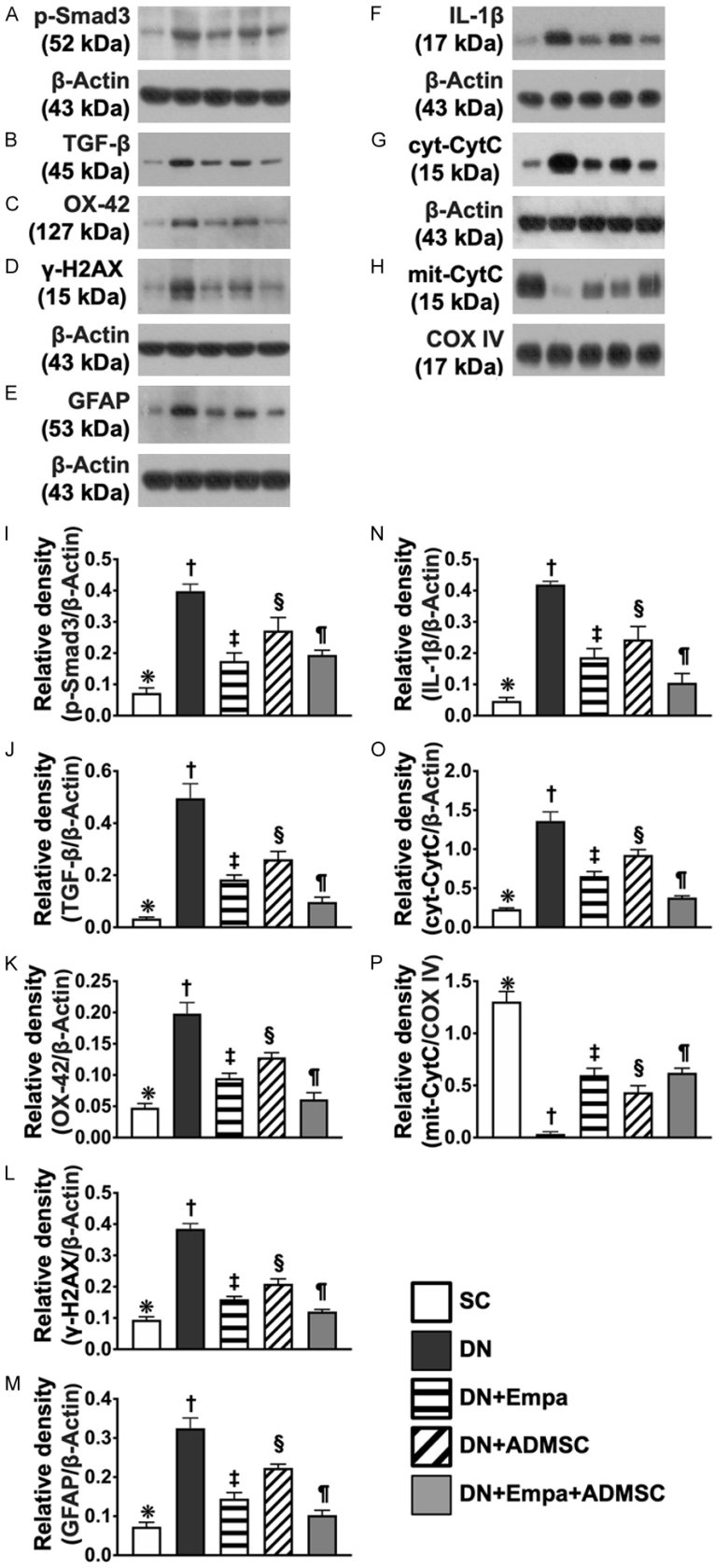

Figure 9. Effect of ADMSCs-empagliflozin therapy on suppressing the protein expressions of fibrosis, mitochondrial/DNA damage and inflammation in L4-L5 levels of DRGs by day 42 after successful DM induction. A and I. Protein expression of phosphorylated (p)-Smad3, * vs. other groups with different symbols (†, ‡, §, ¶), P<0.0001. B and J. Protein expression of transforming growth factor (TGF)-β, * vs. other groups with different symbols (†, ‡, §, ¶), P<0.0001. C and K. Protein expression of OX-42, * vs. other groups with different symbols (†, ‡, §, ¶), P<0.0001. D and L. Protein expression of γ-H2AX, * vs. other groups with different symbols (†, ‡, §, ¶), P<0.0001. E and M. Protein expression of glial fibrillary acidic protein (GFAP), * vs. other groups with different symbols (†, ‡, §, ¶), P<0.0001. F and N. Protein expression of interleukin (IL)-1β, * vs. other groups with different symbols (†, ‡, §, ¶), P<0.0001. G and O. Protein expression of cytosolic cytochrome C (cyt-CytoC), * vs. other groups with different symbols (†, ‡, §, ¶), P<0.0001. H and P. Protein expression of mitochondrial cytochrome C (mit-CytoC), * vs. other groups with different symbols (†, ‡, §, ¶), P<0.0001. All statistical analyses were performed by one-way ANOVA, followed by Bonferroni multiple comparison post hoc test (n = 6 for each group). Symbols (*, †, ‡, §, ¶) indicate significance for each other (at 0.05 level). Group 1 = sham-control (SC); group 2 = diabetic neuropathy (DN); group 3 = DN + Empa; group 4 = DN + allogenic ADMSCs; group 5 = DN + Empa + allogenic ADMSCs. ADMSCs = adipose-derived mesenchymal stem cells; Empa = empagliflozin.

thermal and mechanical stimulations in DN animals through alleviating the oxidative stress, inflammation and pain-facilitated factors in neurons, nerve cells and nervous tissues, resulting in improving the functional integrity of the nervous system.

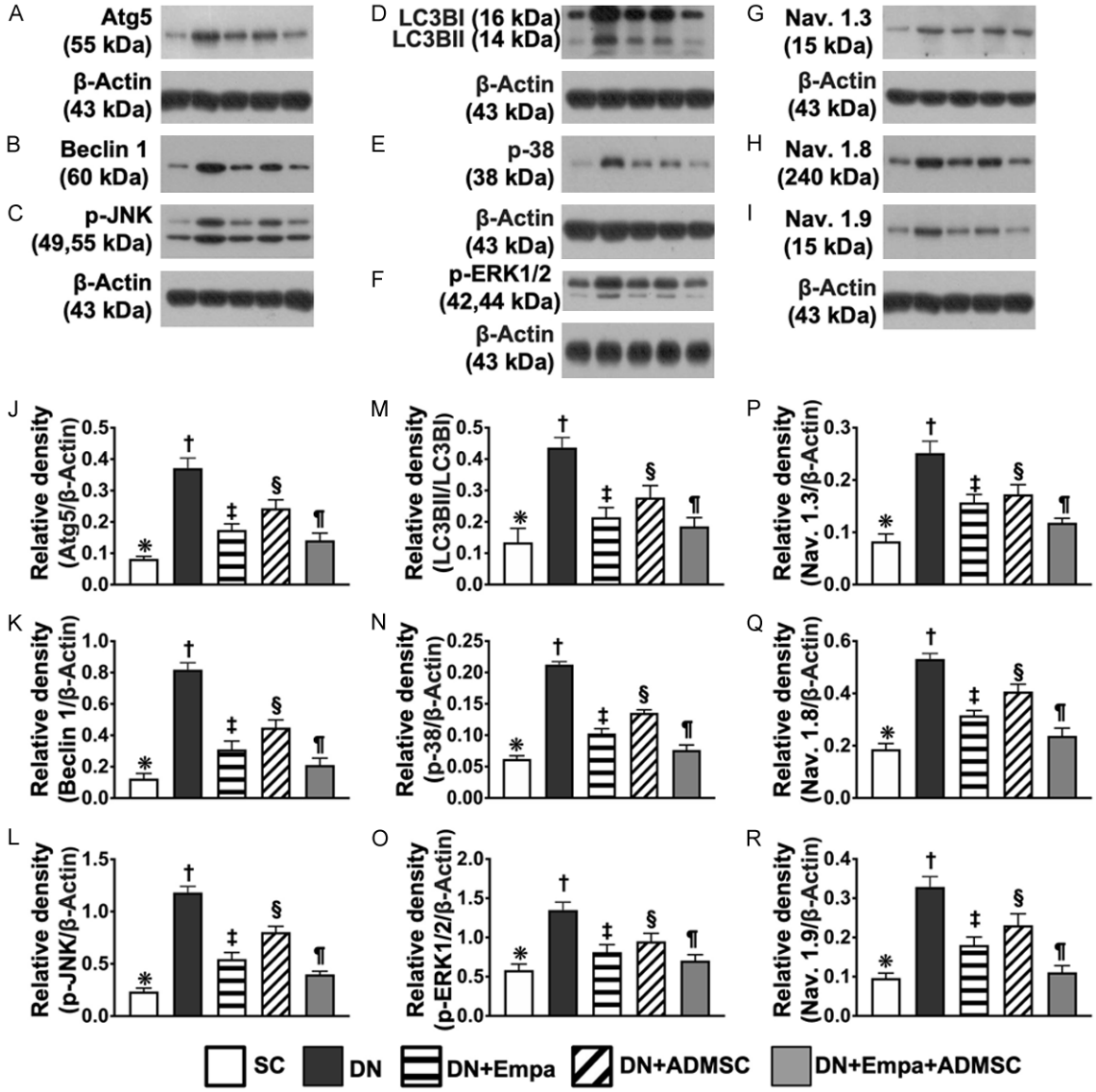

Figure 10. Effect of ADMSCs-empagliflozin therapy on suppressing the protein expressions of autophagy and pain-facilitated biomarkers in L4-L5 level of DRGs by day 42 after successful DM induction. A and J. Protein expression of Atg5, * vs. other groups with different symbols (†, ‡, §, ¶), P<0.0001. B and K. Protein expression of beclin 1, * vs. other groups with different symbols (†, ‡, §, ¶), P<0.0001. C and L. Protein expression of the ratio of LC3B-II to LC3B-I, * vs. other groups with different symbols (†, ‡, §, ¶), P<0.0001. D and M. Protein expression of phosphorylated (p)-P38, * vs. other groups with different symbols (†, ‡, §, ¶), P<0.0001. E and N. Protein expression of p-JNK, * vs. other groups with different symbols (†, ‡, §, ¶), P<0.0001. F and O. Protein expression of p-ERK1/2, * vs. other groups with different symbols (†, ‡, §, ¶), P<0.0001. G and P. Protein expression of Nav.1.3, * vs. other groups with different symbols (†, ‡, §, ¶), P<0.0001. H and Q. Protein expression of Nav.1.8, * vs. other groups with different symbols (†, ‡, §, ¶), P<0.0001. I and R. Protein expression of Nav.1.9, * vs. other groups with different symbols (†, ‡, §, ¶), P<0.0001. All statistical analyses were performed by one-way ANOVA, followed by Bonferroni multiple comparison post hoc test (n = 6 for each group). Symbols (*, †, ‡, §, ¶) indicate significance for each other (at 0.05 level). Group 1 = sham-control (SC); group 2 = diabetic neuropathy (DN); group 3 = DN + Empa; group 4 = DN + allogenic ADMSCs; group 5 = DN + Empa + allogenic ADMSCs. ADMSCs = adipose-derived mesenchymal stem cells; Empa = empagliflozin.

The DN is commonly found in diabetic patients and more than 30% of these patients will develop NP [4]. This clinical setting of hyperglycemia induced NP has been well identified to be reproducible in an animal model [28, 31]. Behavioral tests, i.e., including MPWT and TPWL, are

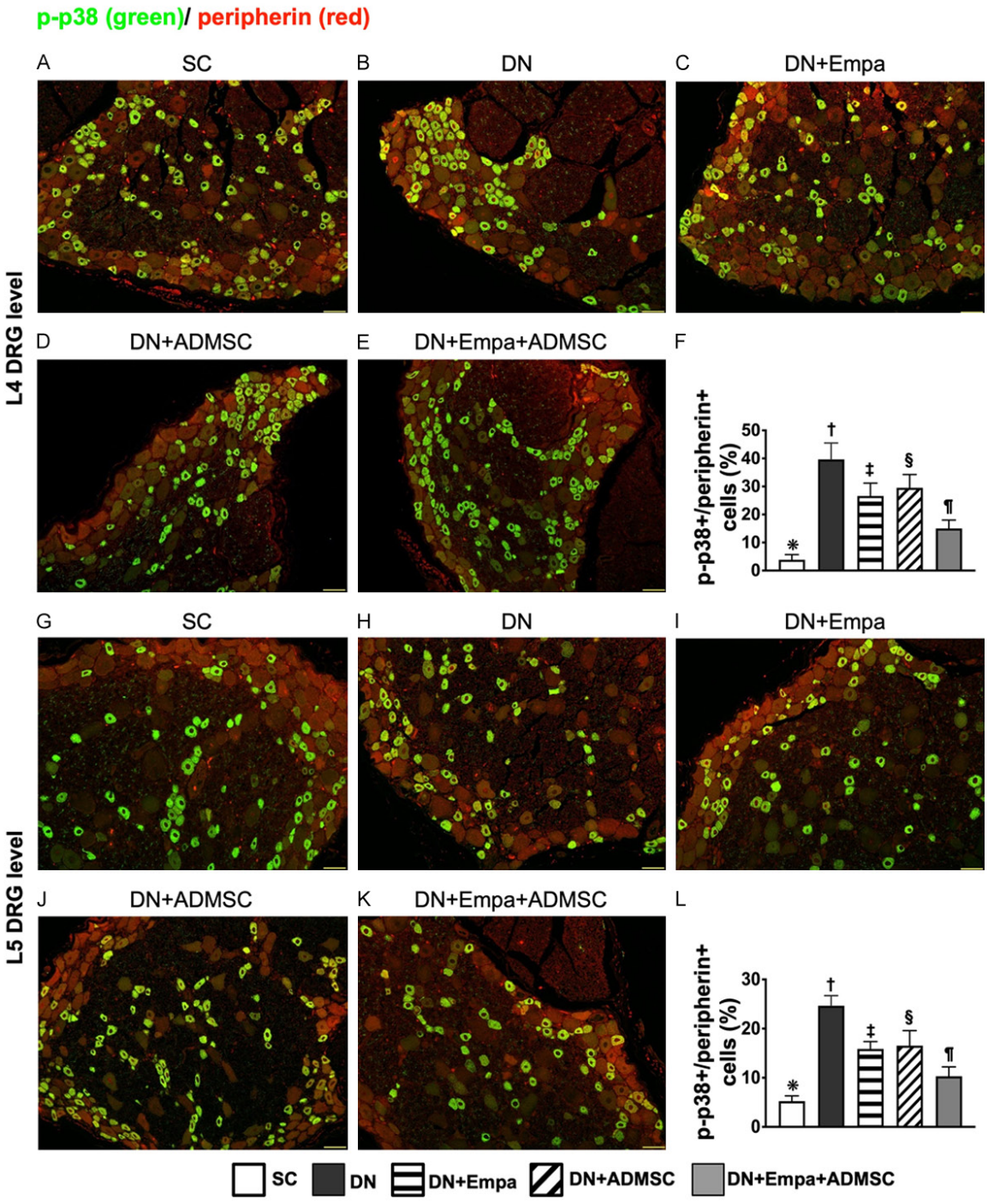

Figure 11. Effect of ADMSCs-empagliflozin therapy on regulating the co-localization of p-P38+ and peripherin+ cells in L4-L5 levels of DRGs by day 42 after successful DM induction. L4 DRG level: A-E. Illustrating the immunofluorescent (IF) microscopic finding (200×) for identifying merged positively-stained p-P38 and peripherin (green-red co-localization cells). F. Analytical results of number of p-P38+/peripherin+ cells, * vs. other groups with different symbols (†, ‡, §, ¶), P<0.0001. L5 DRG level: G-K. Illustrating IF microscopic finding (200×) for identifying merged positively-stained p-P38 and peripherin (green-red co-localization). L. Analytical results of number of p-P38+/peripherin+ cells, * vs. other groups with different symbols (†, ‡, §, ¶), P<0.0001. Scale bars in right lower corner represent 50 μm. All statistical analyses were performed by one-way ANOVA, followed by Bonferroni multiple comparison post hoc test (n = 6-8 for each group). Symbols (*, †, ‡, §, ¶) indicate significance for each other (at 0.05 level). Group 1 = sham-control (SC); group 2 = diabetic neuropathy (DN); group 3 = DN + Empa; group 4 = DN + allogenic ADMSCs; group 5 = DN + Empa + allogenic ADMSCs. ADMSCs = adipose-derived mesenchymal stem cells; Empa = empagliflozin.

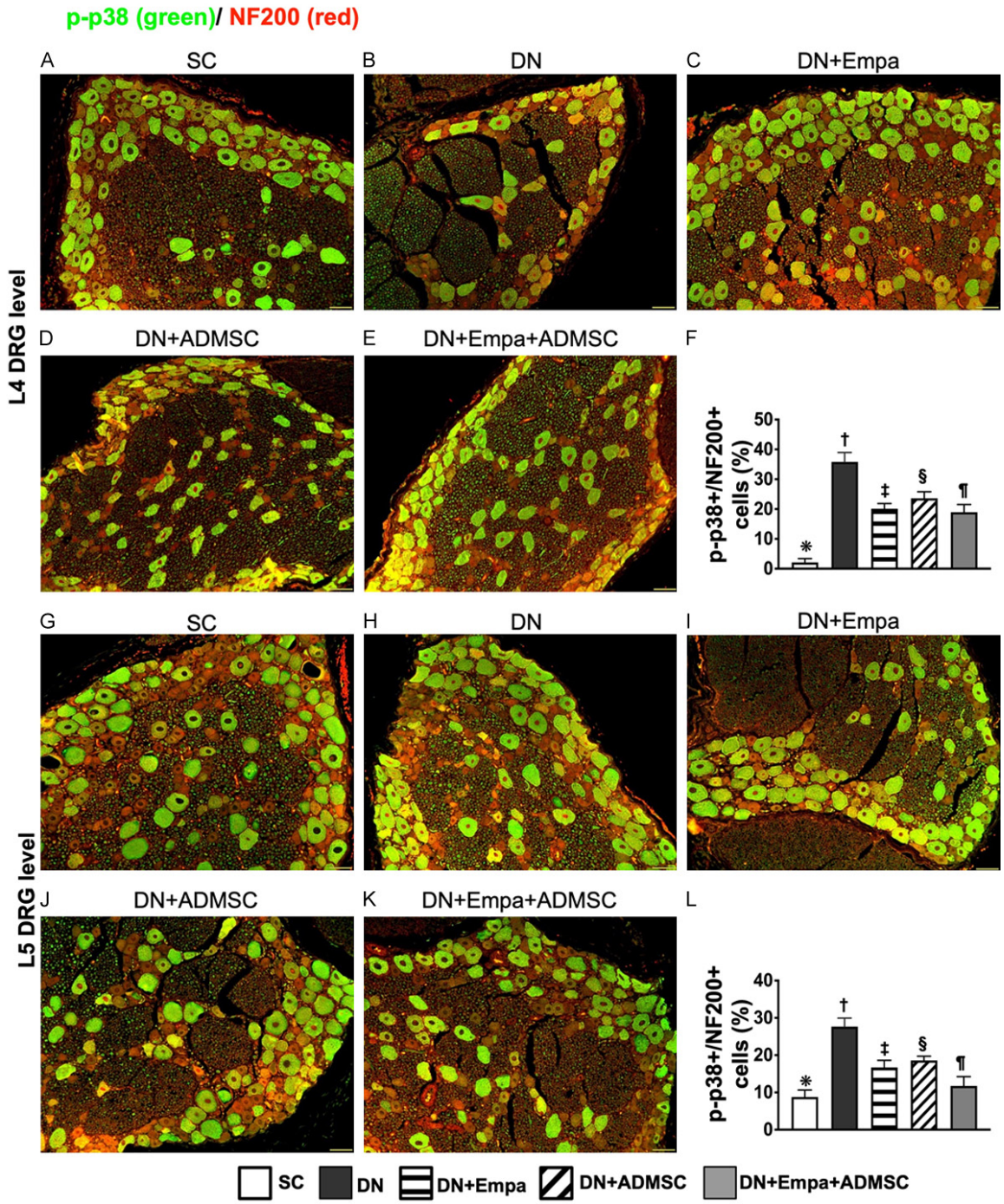

Figure 12. Effect of ADMSCs-empagliflozin therapy on regulating the co-localization of p-P38-NF200 in L4-L5 levels of DRGs by day 42 after successful DM induction. L4-DRG level: A-E. Illustrating the immunofluorescent (IF) microscopic finding (200×) for identifying merged positively-stained p-P38 and NF200 (green-red co-localization cells). F. Analytical results of number of p-P38+/NF200+ cells, * vs. other groups with different symbols (†, ‡, §, ¶), P<0.0001. L5-DRG level: G-K. Illustrating IF microscopic finding (200×) for identifying merged positively-stained p-P38 and NF200 (green-red co-localization cells). L. Analytical results of number of p-P38+/NF200+ cells, * vs. other groups with different symbols (†, ‡, §, ¶), P<0.0001. Scale bars in right lower corner represent 50 μm. All statistical analyses were performed by one-way ANOVA, followed by Bonferroni multiple comparison post hoc test (n = 6-8 for each group). Symbols (*, †, ‡, §, ¶) indicate significance for each other (at 0.05 level). Group 1 = sham-control (SC); group 2 = diabetic neuropathy (DN); group 3 = DN + Empa; group 4 = DN + allogenic ADMSCs; group 5 = DN + Empa + allogenic ADMSCs. ADMSCs = adipose-derived mesenchymal stem cells; Empa = empagliflozin.

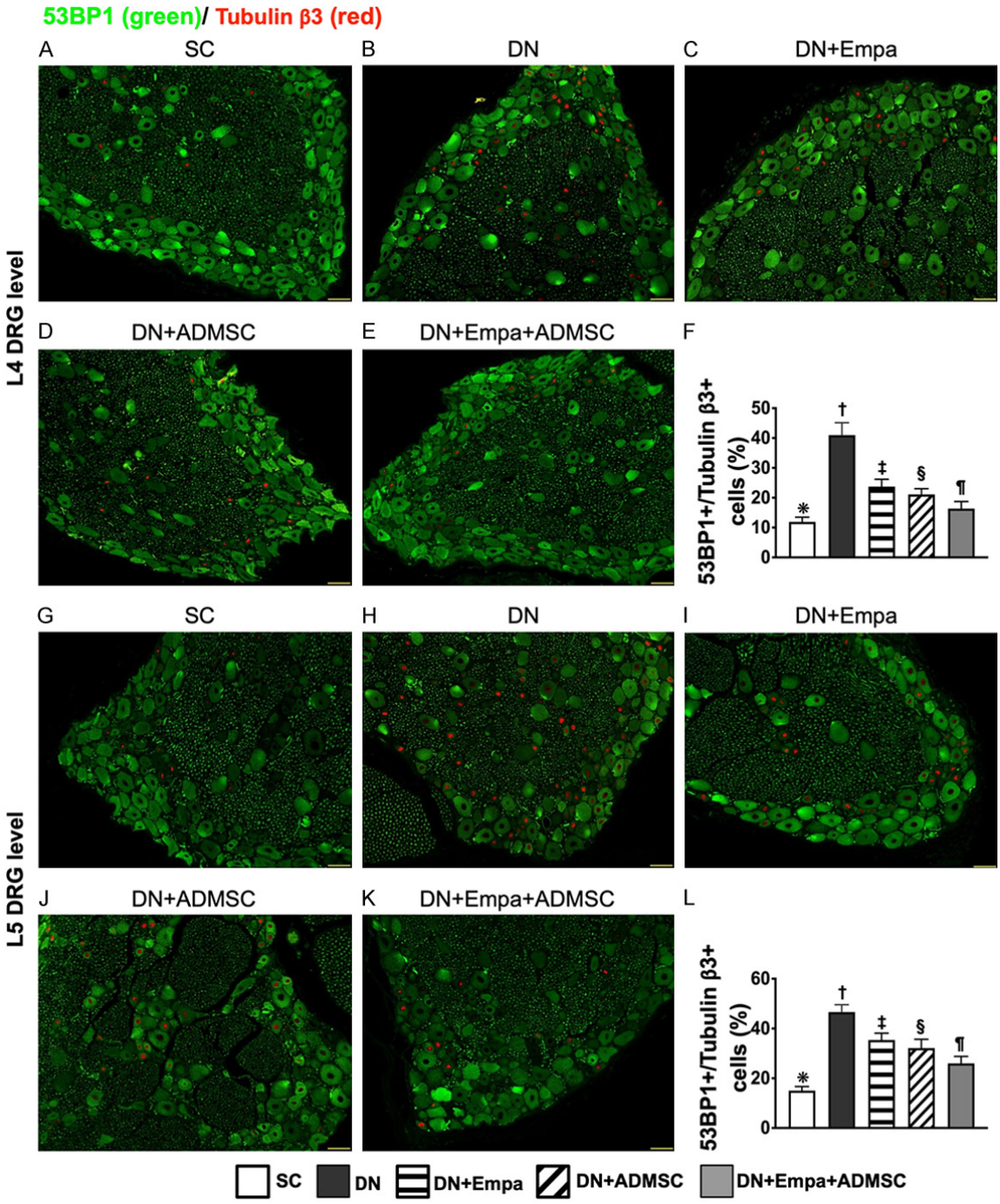

Figure 13. Impact of ADMSCs-empagliflozin therapy on suppressing cellular expression of DNA damage in L4-L5 levels of DRGs by day 42 after successful DM induction. L4-DRG level: A-E. Illustrating (400×) the immunofluorescent (IF) stain for verifying the cellular expression of γ-H2AX (red color). F. Analytical result of number of γ-H2AX+ cells, * vs. other groups with different symbols (†, ‡, §, ¶), P<0.0001. L5-DRG level: G-K. Illustrating IF microscopic finding (200×) for verifying the cellular expression of γ-H2AX (red color). L. Analytical result of number of γ-H2AX+ cells, * vs. other groups with different symbols (†, ‡, §, ¶), P<0.0001. Green color indicated Tubulin β3 stain. Scale bars in right lower corner represent 20 μm. All statistical analyses were performed by one-way ANOVA, followed by Bonferroni multiple comparison post hoc test (n = 6-8 for each group). Symbols (*, †, ‡, §, ¶) indicate significance for each other (at 0.05 level). Group 1 = sham-control (SC); group 2 = diabetic neuropathy (DN); group 3 = DN + Empa; group 4 = DN + allogenic ADMSCs; group 5 = DN + Empa + allogenic ADMSCs. ADMSCs = adipose-derived mesenchymal stem cells; Empa = empagliflozin.

believed to be two of the most sensitive and suitable tools for pain tolerance in the animal world [11, 12]. The most important finding in the present study was that as compared with the SC the thresholds of MPWT and TPWL were remarkably abnormally increased in DN animals, i.e., diminished the sensitive to the thermal and mechanical stimulations. In this way, our finding could explain why the DN patients always ignore hot situation, resulting in thermal or mechanical damage. Importantly, these two pain thresholds corresponding to the minimum intensity at which an animal began to perceive pain were remarkably downregulated in DN animals with as compared to those of DN animals without ADMSCs or EMPA therapy. Of particular importance was that combined ADMSCs and EMPA therapy was superior to merely one therapy for suppressing the abnormally elevated MPWT and TPWL thresholds in DN animals, highlighting that this innovative treatment could have great therapeutic potential for the DN patients, especially for those who are always refractory to conventional medical therapy.

Undoubtedly, persistent hyperglycemia frequently elicited the molecular-cellular perturbations, including inflammatory reaction, oxidative stress, apoptosis and fibrosis in damaged or even non-damaged tissues and organs [35, 36]. An essential finding in the in vitro study was that hyperglycemia not only upregulated the aforementioned molecular-cellular perturbations but also enhanced the apoptosis, fibrosis, DNA/mitochondrial damage and autophagy in N2a cells. Consistently, these molecular-cellular perturbations were also identically found in the in vivo study. Accordingly, our findings, in addition to being consistent with the findings of the previous studies [35, 36], could partially explain why the abnormally elevated MPWT and TPWL thresholds were substantially upregulated in DN animals than in those of the SC animals. However, these molecular-cellular perturbations in DN animals were markedly reversed in ADMSCs or EMPA treatment and furthermore reversed by combined ADMSCs-EMPA treatment could, at least in part, explain why the abnormally elevated MPWT and TPWL thresholds were significantly downregulated by the ADMSCs or empagliflozin treatment and further notably downregulated by combined ADMSCs and empagliflozin treatment in DN animals.

MAPK family signaling and voltage-gated sodium channels have clearly identified to play an important role on facilitating the painful sensation, i.e., lowering the tolerance of pain sensitivity [11, 12]. Principal finding in the present study was that the parameters of MAPK family signaling (i.e., p-P38, p-JNK, p-ERK1/2) and biomarkers of voltage-gated sodium channels (Nav.1.3/Nav.1.8/Nav.1.9) were remarkably upregulated in DN animals, suggesting that these painful facilitated biomarkers were commonly upregulated in dysesthesia (i.e., marked loss of pain sensations) our DN animals. This finding could be explained as that the symptoms of DN are actually categorized into (1) paresthesia (numbness), (2) allodynia, (3) hyperalgesia (lower pain threshold), and (4) dysesthesia (loss of pain sensations), respectively [37]. Based on the findings of MPWT and TPWL in the present study, we proposed that the DN rodents in the present study could, perhaps, be categorized in the group of dysesthesia and the painful facilitated biomarkers which were upregulated could be an intrinsic response to the thermal and mechanical stimulation that were significantly alleviated by ADMSCs or EMPA therapy and furthermore significantly alleviated by combined ADMSCs and EMPA therapy.

Study limitations

This study has limitations. First, although the study period was 42 days after DM induction, it could be still relatively shorter when an enough time interval of development of DN-induced neurologic complication was taken into consideration. Second, the possibility of other major organ complications, such as cardiovascular disease, cerebrovascular disease or chronic kidney disease had not been investigated in the current study.

Conclusions

The study demonstrated that persistent hyperglycemia induced hyperglycemic neuropathy that was effectively alleviated by ADMSC or EMPA therapy and more effectively alleviated by combining these two regimens.

Acknowledgements

This research was supported by a program grant from Chang Gung Memorial Hospital, Chang Gung University (CMRPG8L0361).

Disclosure of conflict of interest

None.

Address correspondence to: Dr. Hon-Kan Yip, Division of Cardiology, Department of Internal Medicine, Kaohsiung Chang Gung Memorial Hospital, No. 123 Dapi Road, Niaosung District, Kaohsiung 83301, Taiwan. Tel: +886-7-7317123 Ext. 8300; Fax: +886-7-7322402; E-mail: han.gung@msa.hinet.net; hkyip@cgmh.org.tw; Dr. Kuan-Hung Chen, Department of Anesthesiology, Kaohsiung Chang Gung Memorial Hospital, No. 123 Dapi Road, Niaosung District, Kaohsiung 83301, Taiwan. Tel: +886-7-7317123 Ext. 2788; Fax: +886-7-7317123 Ext. 2791; E-mail: amigofx35@gmail.com; amigo6463@cgmh.org.tw

References

[1] Cho NH, Shaw JE, Karuranga S, Huang Y, da Rocha Fernandes JD, Ohlrogge AW and Malanda B. IDF Diabetes Atlas: global estimates of diabetes prevalence for 2017 and projections for 2045. Diabetes Res Clin Pract 2018; 138: 271-281.

[2] Feldman EL, Callaghan BC, Pop-Busui R, Zochodne DW, Wright DE, Bennett DL, Bril V, Russell JW and Viswanathan V. Diabetic neuropathy. Nat Rev Dis Primers 2019; 5: 42.

[3] Tabish SA. Is diabetes becoming the biggest epidemic of the twenty-first century? Int J Health Sci (Qassim) 2007; 1: V-VIII.

[4] Abbott CA, Malik RA, van Ross ER, Kulkarni J and Boulton AJ. Prevalence and characteristics of painful diabetic neuropathy in a large community-based diabetic population in the U.K. Diabetes Care 2011; 34: 2220-2224.

[5] Boyle J, Eriksson ME, Gribble L, Gouni R, Johnsen S, Coppini DV and Kerr D. Randomized, placebo-controlled comparison of amitriptyline, duloxetine, and pregabalin in patients with chronic diabetic peripheral neuropathic pain: impact on pain, polysomnographic sleep, daytime functioning, and quality of life. Diabetes Care 2012; 35: 2451-2458.

[6] Finnerup NB, Attal N, Haroutounian S, McNicol E, Baron R, Dworkin RH, Gilron I, Haanpaa M, Hansson P, Jensen TS, Kamerman PR, Lund K, Moore A, Raja SN, Rice AS, Rowbotham M, Sena E, Siddall P, Smith BH and Wallace M. Pharmacotherapy for neuropathic pain in adults: a systematic review and meta-analysis. Lancet Neurol 2015; 14: 162-173.

[7] Dowell D, Haegerich TM and Chou R. CDC guideline for prescribing opioids for chronic pain--United States, 2016. JAMA 2016; 315: 1624-1645.

[8] Franklin GM; American Academy of Neurology. Opioids for chronic noncancer pain: a position paper of the American Academy of Neurology. Neurology 2014; 83: 1277-1284.

[9] Figueroa-Romero C, Sadidi M and Feldman EL. Mechanisms of disease: the oxidative stress theory of diabetic neuropathy. Rev Endocr Metab Disord 2008; 9: 301-314.

[10] Roman-Pintos LM, Villegas-Rivera G, Rodriguez-Carrizalez AD, Miranda-Diaz AG and Cardona-Munoz EG. Diabetic polyneuropathy in type 2 diabetes mellitus: inflammation, oxidative stress, and mitochondrial function. J Diabetes Res 2016; 2016: 3425617.

[11] Chen KH, Yang CH, Wallace CG, Lin CR, Liu CK, Yin TC, Huang TH, Chen YL, Sun CK and Yip HK. Combination therapy with extracorporeal shock wave and melatonin markedly attenuated neuropathic pain in rat. Am J Transl Res 2017; 9: 4593-4606.

[12] Yang CH, Yip HK, Chen HF, Yin TC, Chiang JY, Sung PH, Lin KC, Tsou YH, Chen YL, Li YC, Huang TH, Huang CR, Luo CW and Chen KH. Long-term therapeutic effects of extracorporeal shock wave-assisted melatonin therapy on mononeuropathic pain in rats. Neurochem Res 2019; 44: 796-810.

[13] Dewanjee S, Das S, Das AK, Bhattacharjee N, Dihingia A, Dua TK, Kalita J and Manna P. Molecular mechanism of diabetic neuropathy and its pharmacotherapeutic targets. Eur J Pharmacol 2018; 833: 472-523.

[14] Mizukami H and Yagihashi S. Exploring a new therapy for diabetic polyneuropathy - the application of stem cell transplantation. Front Endocrinol (Lausanne) 2014; 5: 45.

[15] Oses C, Olivares B, Ezquer M, Acosta C, Bosch P, Donoso M, Leniz P and Ezquer F. Preconditioning of adipose tissue-derived mesenchymal stem cells with deferoxamine increases the production of pro-angiogenic, neuroprotective and anti-inflammatory factors: potential application in the treatment of diabetic neuropathy. PLoS One 2017; 12: e0178011.

[16] Prockop DJ, Kota DJ, Bazhanov N and Reger RL. Evolving paradigms for repair of tissues by adult stem/progenitor cells (MSCs). J Cell Mol Med 2010; 14: 2190-2199.

[17] Keilhoff G, Stang F, Goihl A, Wolf G and Fansa H. Transdifferentiated mesenchymal stem cells as alternative therapy in supporting nerve regeneration and myelination. Cell Mol Neurobiol 2006; 26: 1235-1252.

[18] Caplan AI and Dennis JE. Mesenchymal stem cells as trophic mediators. J Cell Biochem 2006; 98: 1076-1084.

[19] Kim WS, Park BS, Kim HK, Park JS, Kim KJ, Choi JS, Chung SJ, Kim DD and Sung JH. Evidence supporting antioxidant action of adi-

pose-derived stem cells: protection of human dermal fibroblasts from oxidative stress. J Dermatol Sci 2008; 49: 133-142.
[20] Prockop DJ and Oh JY. Mesenchymal stem/stromal cells (MSCs): role as guardians of inflammation. Mol Ther 2012; 20: 14-20.
[21] Frampton JE. Empagliflozin: a review in type 2 diabetes. Drugs 2018; 78: 1037-1048.
[22] Zinman B, Inzucchi SE, Lachin JM, Wanner C, Ferrari R, Fitchett D, Bluhmki E, Hantel S, Kempthorne-Rawson J, Newman J, Johansen OE, Woerle HJ and Broedl UC. Rationale, design, and baseline characteristics of a randomized, placebo-controlled cardiovascular outcome trial of empagliflozin (EMPA-REG OUTCOME™). Cardiovasc Diabetol 2014; 13: 102.
[23] Fitchett D, Zinman B, Wanner C, Lachin JM, Hantel S, Salsali A, Johansen OE, Woerle HJ, Broedl UC and Inzucchi SE; EMPA-REG OUTCOME® trial investigators. Heart failure outcomes with empagliflozin in patients with type 2 diabetes at high cardiovascular risk: results of the EMPA-REG OUTCOME(R) trial. Eur Heart J 2016; 37: 1526-1534.
[24] Kadowaki T, Nangaku M, Hantel S, Okamura T, von Eynatten M, Wanner C and Koitka-Weber A. Empagliflozin and kidney outcomes in Asian patients with type 2 diabetes and established cardiovascular disease: results from the EMPA-REG OUTCOME((R)) trial. J Diabetes Investig 2019; 10: 760-770.
[25] Scott LJ. Empagliflozin: a review of its use in patients with type 2 diabetes mellitus. Drugs 2014; 74: 1769-1784.
[26] Steven S, Oelze M, Hanf A, Kroller-Schon S, Kashani F, Roohani S, Welschof P, Kopp M, Godtel-Armbrust U, Xia N, Li H, Schulz E, Lackner KJ, Wojnowski L, Bottari SP, Wenzel P, Mayoux E, Munzel T and Daiber A. The SGLT2 inhibitor empagliflozin improves the primary diabetic complications in ZDF rats. Redox Biol 2017; 13: 370-385.
[27] Yang CC, Chen YT, Wallace CG, Chen KH, Cheng BC, Sung PH, Li YC, Ko SF, Chang HW and Yip HK. Early administration of empagliflozin preserved heart function in cardiorenal syndrome in rat. Biomed Pharmacother 2019; 109: 658-670.
[28] Chen YL, Chen KH, Yin TC, Huang TH, Yuen CM, Chung SY, Sung PH, Tong MS, Chen CH, Chang HW, Lin KC, Ko SF and Yip HK. Extracorporeal shock wave therapy effectively prevented diabetic neuropathy. Am J Transl Res 2015; 7: 2543-2560.
[29] Yue Y, Yeh JN, Chiang JY, Sung PH, Chen YL, Liu F and Yip HK. Intrarenal arterial administration of human umbilical cord-derived mesenchymal stem cells effectively preserved the residual renal function of diabetic kidney disease in rat. Stem Cell Res Ther 2022; 13: 186.
[30] Yang CC, Sung PH, Chen KH, Chai HT, Chiang JY, Ko SF, Lee FY and Yip HK. Valsartan- and melatonin-supported adipose-derived mesenchymal stem cells preserve renal function in chronic kidney disease rat through upregulation of prion protein participated in promoting PI3K-Akt-mTOR signaling and cell proliferation. Biomed Pharmacother 2022; 146: 112551.
[31] Chen KH, Lin HS, Li YC, Sung PH, Chen YL, Yin TC and Yip HK. Synergic effect of early administration of probiotics and adipose-derived mesenchymal stem cells on alleviating inflammation-induced chronic neuropathic pain in rodents. Int J Mol Sci 2022; 23: 11974.
[32] Sung PH, Sun CK, Ko SF, Chang LT, Sheu JJ, Lee FY, Wu CJ, Chua S and Yip HK. Impact of hyperglycemic control on left ventricular myocardium. A molecular and cellular basic study in a diabetic rat model. Int Heart J 2009; 50: 191-206.
[33] Ko SF, Huang TH, Lin YP, Chen YL and Yip HK. Accuracy and precision of 31P-MRS assessment for evaluating the effect of melatonin-pretreated mitochondria transferring on liver fibrosis of rats. Melatonin Research 2022; 5: 18-33.
[34] Bennett DL, Clark AJ, Huang J, Waxman SG and Dib-Hajj SD. The role of voltage-gated sodium channels in pain signaling. Physiol Rev 2019; 99: 1079-1151.
[35] Jia W, Bai T, Zeng J, Niu Z, Fan D, Xu X, Luo M, Wang P, Zou Q and Dai X. Combined administration of metformin and atorvastatin attenuates diabetic cardiomyopathy by inhibiting inflammation, apoptosis, and oxidative stress in type 2 diabetic mice. Front Cell Dev Biol 2021; 9: 634900.
[36] Papachristoforou E, Lambadiari V, Maratou E and Makrilakis K. Association of glycemic indices (hyperglycemia, glucose variability, and hypoglycemia) with oxidative stress and diabetic complications. J Diabetes Res 2020; 2020: 7489795.
[37] Alsunousi S and Marrif HI. Diabetic neuropathy and the sensory apparatus "meissner corpuscle and merkel cells". Front Neuroanat 2014; 8: 79.

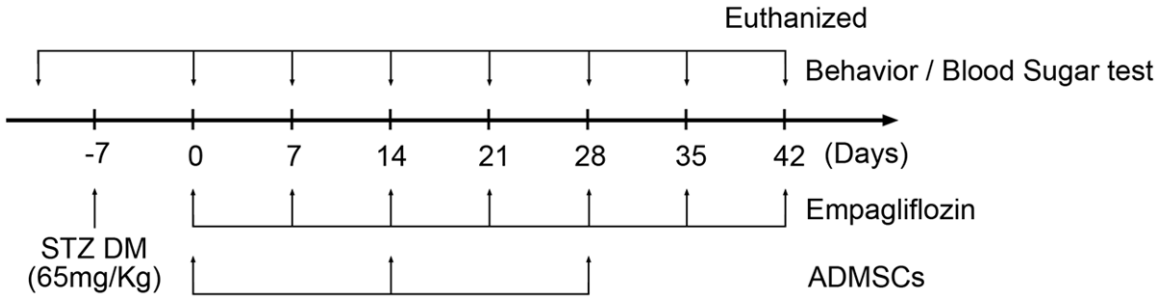

Supplementary Figure 1. Illustrates the time point of DM induction, time intervals of treatment and the time courses of blood sugar and neurological behavior examinations. DM = diabetes mellitus; ADMSCs = adipose-derived mesenchymal stem cells; STZ = streptozocin.